International Journal of Tumor Therapy 2018, 7(1): 1-26
DOI: 10.5923/j.ijtt.20180701.01

A Computational Assessment of the Robustness of Cancer Treatments with Respect to Immune Response Strength, Tumor Size and Resistance

Michael Fernandez[1], Mingyan Zhou[2], Luis Soto-Ortiz[3,*]

[1]Department of Molecular and Cell Biology, University of California, Berkeley, USA
[2]Department of Mathematics, University of California, Los Angeles, USA
[3]Department of Mathematics, East Los Angeles College, Monterey Park, USA

Abstract The emergence of bioengineering has paved the way for the *in vitro* design of immune cells that can detect and destroy tumor cells of low antigenicity. However, the results of clinical trials involving cancer treatments have not matched the success in the lab. A reason for treatment failure is the presence of patient-specific genetic biomarkers that affect long-term effectiveness. The cross-talk between multiple signaling pathways involved in tumor cell survival, the existence of redundant pathways with similar functions, and the intrinsic genetic instability of tumor cells also contribute to treatment failure. With the advent of novel cancer treatments, a need has arisen to undertake a computational approach to identify treatment combinations that maximize long-term effectiveness while minimizing the risk of serious side effects. In the present work, mathematical modeling was used to track the time-varying concentrations of pro- and anti-tumor cells and cytokines after a cancer treatment is administered. The simulations demonstrated the importance of treatment timing and frequency to achieve synergy. A combination therapy based on sunitinib and fresolimumab was found to be robust in reducing tumor size with respect to the strength of a patient's anti-tumor immune response, the size of the tumor at the start of treatment, and with respect to mutations that can make cancer cells become refractory to the first-line treatment. The robustness of the identified sunitinib + fresolimumab combination therapy confers it with the capability to eliminate heterogeneous tumors made up of sensitive and resistant cells, in a patient whose anti-tumor immune response has become suppressed due to advanced age, chronic inflammation or a prior medical treatment. The model simulations highlight the superiority of combination therapy over monotherapy, and provide guidance to identify protocols that have the greatest potential to eliminate a tumor.

Keywords Monoclonal antibody, Immunotherapy, Mathematical modeling, Angiogenesis, Robustness

1. Introduction

In spite of our increasingly deeper understanding of cancer biology, designing an effective treatment has proven difficult. Reasons for the shortcomings of cancer treatments include the complexity of the genetic entropy of the networks involved [1-3], the genetic differences between same-site cancer patients that determine their distinct sensitivities to the same type of therapy [4], the inability of cancer cells to repair DNA damage that increases their genetic instability and their resistance to treatment [5-7], and the risk of harmful side effects [8-11]. The therapeutic potential of various treatment modalities, as well as their shortcomings, will now be reviewed.

* Corresponding author:
sotoorLf@elac.edu (Luis Soto-Ortiz)
Published online at http://journal.sapub.org/ijtt

1.1. Chemotherapy

Chemotherapy was one of the first cancer treatments to be widely adopted [12]. Chemotherapy seemed to be an ideal treatment for cancer, since cancer cells exhibit a high replication rate and chemotherapy drugs mainly disrupt the genetic networks of cells that replicate at a fast rate. Depending on the chemotherapy agent that is used, the mechanism of action may include the inhibition of topoisomerase I, leading to its inability to remove DNA supercoils that block cell replication, or the inhibition of topoisomerase II, leading to DNA breakage that remains unrepaired [13-15]. This results in the arrest of tumor cells at some stage of the cell cycle, leading to their eventual death. Chemotherapy has proven useful in reducing the growth rate of certain types of cancer. As an adjuvant therapy following surgery or radiotherapy, chemotherapy can eliminate most, if not all, remaining cancer cells as long as resistance does not develop.

Since healthy cells also replicate, albeit at a lower rate, they are also susceptible to the same cytotoxic effects experienced by cancer cells due to the non-targeted mechanism of action of chemotherapy. This cytotoxicity on healthy somatic and immune cells is a key factor that limits the therapeutic effect of chemotherapy in a clinical setting. Another obstacle to a successful elimination of a tumor is the emergence of mutant tumor cells that are resistant to chemotherapy [16, 17]. Once mutant cells develop, they are able to escape the cytotoxic effect of chemotherapy, leading to treatment failure.

1.2. Monoclonal Antibody Therapy

A more recent mode to treat cancer involves the application of humanized monoclonal antibodies (mAbs). Monoclonal antibodies originate from a single cell line and thus have the same molecular shape and function. They act like naturally produced antibodies and are engineered to attach with high affinity to specific molecular targets found in the membrane of cancer cells. Monoclonal antibodies can also bind to cytokines, blocking their pro-tumor activity. Examples of mAbs that have been used to treat cancer include bevacizumab, which targets the Vascular Endothelial Growth Factor (VEGF) [18, 19], fresolimumab, which targets the Tumor Growth Factor-beta (TGF-β) [20, 21], trastuzumab, cetuximab and panitumumab, all of which target the Epidermal Growth Factor (EGFR) and the Human Epidermal Growth Factor Receptor 2 (HER2) [22, 23] and vitaxin, which targets the alpha-v beta-3 ($\alpha v \beta 3$) integrin found in endothelial cells [24, 25].

The tumor microenvironment is typically immunosuppressive and, consequently, attenuates the anti-tumor response of the innate, adaptive and humoral arms of the immune system, allowing the tumor cells to escape destruction. Monoclonal antibodies have been engineered to block the immunosuppressive activity of pro-tumor cells such as regulatory T cells, M2 macrophages, Th2 helper cells, and myeloid-derived suppressor cells (MDSC). Other mAbs are designed to disrupt signaling networks involving immunosuppressive cytokines such as VEGF, TGF-β, and IL-10. Monoclonal antibodies that reduce immunosuppression include sunitinib, which is a tyrosine kinase inhibitor that eliminates the immunosuppression caused by regulatory T cells (Treg cells) and by MDSC [26-28]. Due to the multi-faceted role of certain cytokines involved in tumor growth, treatments involving sunitinib, bevacizumab, trastuzumab, and cetuximab are able to disrupt signaling networks that simultaneously enhance tumor angiogenesis and immunosuppression.

Therapies based on monoclonal antibodies have limitations that diminish their therapeutic impact. A disadvantage of this mode of treatment is the high manufacturing cost of antibodies [29, 30]. A second limitation is the fact that monoclonal antibodies are large molecules that tend to interact with receptors of healthy cells, keeping the antibodies from reaching the tumor site quickly and in large numbers. Their high affinity for the target molecule means that mAbs strongly bind to their target on the first encounter and fail to penetrate deep into the tumor [31]. Heterogeneous tumor vascularization also affects antibody penetration [32]. This limited penetration spares many malignant cells and reduces the effectiveness of mAb-based treatments. The problem of pharmacokinetics versus tissue penetration is typical of monoclonal antibodies and is a major drawback of this mode of treatment. Moreover, once mAbs are infused into a patient, resistance to mAb monotherapy usually emerges over time and/or intolerable side effects occur [33, 34]. The outcome of a mAb treatment also depends on the type of mutations that are already present in the tumor cells, or that develop during the course of treatment. For example, anti-EGFR treatments such as cetuximab and panitumumab are known to be ineffective if KRAS mutations are present in tumor cells [35, 36].

A combination of cetuximab and small molecule tyrosine kinase inhibitors (TKIs) can lead to an enhanced inhibition of EGFR autophosphorylation [37], increasing the effectiveness of this combination therapy. For some cancers, combining cetixumab or panitumumab with chemotherapy also appears to be a promising approach [38]. For example, the cytotoxicity of irinotecan chemotherapy is enhanced when it is combined with cetuximab or panitumumab through a chemosensitization of tumor cells [39]. However, due to the emergence of resistance to irinotecan, cetuximab and panitumumab [40-43], the therapeutic effect of a combination therapy that involves these drugs is limited.

1.3. Therapy that Boosts the Immune Response

A third category of anti-cancer treatments includes approaches that boost the anti-tumor immune response and increase the antigenicity of the tumor. Molecule-based treatments involve the injection of tumor cell antigens or of toll-like receptor (TLR) agonists. TLR agonists strengthen immune-cell functions by enhancing antigen-presentation of dendritic cells (DC) [44], by steering the polarization of macrophages into M1 macrophages [45], and the polarization of naïve CD4+ T cells into Th1 helper cells [46]. Cytokine-based treatments that have been shown to be successful in boosting the anti-tumor immune response involve the injection of anti-tumor interleukins (IL-2 and IL-12) or interferons (IFN-α, IFN-β) [47-50], which activate CD8+ cytotoxic T lymphocytes (CTL), natural killer (NK) cells, and macrophages, and promote their expansion and anti-tumor activity.

Cell-based therapies aimed at boosting the cytotoxic immune response involve the extraction of live CTL or NK cells from the patient, expanding them and priming them in vitro to make them more reactive to tumor antigens. An enhanced sensitivity by immune cells can be achieved by exposing them in vitro to IL-2 and to antigenic molecules found in the membrane of cancer cells. The CTL or NK

cells are then infused back into the patient via an intravenous injection or directly into the tumor site. This type of treatment is known as adoptive cell transfer (ACT) [51-54]. The infused immune cells are capable of sensing and penetrating the tumor, enhancing their tumor-targeted cytotoxic activity. When tumor cells are of a very low antigenicity such that no tumor antigens are present in their membrane, adoptive immune cells can be genetically engineered in vitro to express chimeric antigen receptors (CARs) [55] that allow them to detect specific proteins found in the membrane of cancer cells. Once activated and expanded, the engineered immune cells are reintroduced into the patient and a strong tumor-targeted immune reaction occurs [56, 57].

In a clinical setting, adoptive cell transfer has been moderately successful for a limited number of cancer types. Regardless of whether adoptive cell transfer involves CTL cells, NK cells or dendritic cells, once these cells are infused into the patient and reach the solid tumor site, they experience a strongly immunosuppressive tumor microenvironment and become anergic or develop a pro-tumor phenotype over time. The result is a short-lived anti-tumor immune reaction that eventually becomes ineffective at arresting tumor growth. To counteract the effect of immunosuppression, a mAb treatment that targets TGF-β, VEGF, or IL-10, or that targets Treg cells directly can be administered before adoptive cell therapy is given. Experimental work shows that administering chemotherapy to reduce immunosuppression before giving ACT is beneficial [58-60]. In adoptive cell transfer, chemotherapy can also be given with the purpose of depleting CD8+ T lymphocytes before infusing NK cells. This lymphodepletion reduces the competition between the infused cells and the anergic lymphocytes for survival and growth signals from anti-tumor interleukins. Infused T cells known as TRUCKs have been engineered to express a 4th generation CAR which allows them to deliver a payload that can modify the tumor microenvironment [61]. TRUCKs are currently being engineered to help reduce the typically immunosuppressive microenvironment of solid tumors [62, 63].

1.4. A Tumor is a Complex Robust System

The limited success of cancer treatments can be attributed to the fact that a tumor is a robust biological system that is able to perform its proliferative function in spite of attempts to eliminate it. In this article, robustness is defined in the same way that Hiroaki Kitano defined it: "Robustness is a property that allows a system to maintain its functions against internal and external perturbations." [64] The study of cancer biology makes it clear that cancer is a disease governed by complex biological networks [65]. The inherent complexity and redundancy of the network connectivity makes cancer growth robust against internal and external perturbations (hypoxia, limited metabolic processes, cancer treatments, etc.). Through the stimulation of angiogenesis, a tumor adapts to a shortage of nutrients and continues to grow successfully after it reaches the diffusion-limited size of 1 million cells, or approximately 1 mm in radius [66]. Through up-regulation of glycolytic processes, a growing tumor successfully bypasses the slow production, through normal metabolic processes, of the required building-block molecules. To effectively disrupt the growth dynamics of such a robust biological system, a therapy that is robust in its own right with respect to changes in tumor cell characteristics and to the level of a patient's immune system response, is required. A mounting set of evidence obtained from experimental work and clinical trials seems to suggest that a combination therapy has the potential to be more robust than monotherapy alone against the changing characteristics of a tumor and its microenvironment. In this regard, mathematical modeling can help to assess and quantify the robustness, or lack thereof, of current therapies. Computational work can also help to identify ways to maximize the robustness of a combination therapy by achieving synergism between its components through proper dose selection and timing.

1.5. Previous Mathematical Models

Previous models of tumor growth have simulated tumor angiogenesis [67-71], the interaction between tumor cells and the immune system [72-74], immunosuppression [75, 76], combination therapy [77-79], and the emergence of resistance to treatment [80-82]. However, models of tumor growth have not simulated a diverse set of treatments, and those that did left out important processes such as angiogenesis, immunosuppression and/or treatment resistance. The present model aims to provide a more comprehensive analysis of a diverse set of therapies while considering key biological processes that influence tumor growth. The parameter sensitivity analyses of previous models have shown that initial tumor size, the maximal tumor growth rate, tumor antigenicity and immune cell cytotoxicity on tumor cells are the main factors that influence treatment success [83-85]. These results motivated the authors to investigate whether combining certain types of treatment leads to a synergistic effect that makes the combination therapy robust in reducing tumor size, with respect to the strength of a patient's anti-tumor immune response, tumor size at the start of treatment, and the emergence of resistance to treatment.

2. Materials and Methods

Our model builds upon the work of [86] and [87]. De Pillis et al. developed a validated model of colorectal cancer consisting of ordinary differential equations (ODE) that considers multiple immune cell types (CD8+ T cells, NK cells and circulating CD4+ T lymphocytes). In their work, they considered chemotherapy (irinotecan) and monoclonal antibodies (cetuximab and panitumumab) as anti-tumor treatments. They investigated the effect of the level of

strength of the anti-tumor immune response on the effectiveness of monotherapy and combination therapy in reducing tumor growth. They also simulated experimental dosing schedules that reduced tumor size more effectively than standard protocols. However, key processes that were not included in their model of colorectal cancer are tumor angiogenesis, immunosuppression due to Treg cells and tumor-secreted cytokines, and the emergence of treatment resistance. To simulate the effect of resistance to treatment, the model in [87] assumed the presence of KRAS-mutant tumor cells prior to treatment. A KRAS mutation eliminates the chemosensitization of tumor cells to irinotecan chemotherapy caused by the injection of cetuximab and panitumumab, and eliminates tumor death caused by direct interaction with the injected mAbs. Their model, however, did not consider tumor vasculature or the immunosuppressive effect of pro-tumor cells and cytokines.

The model expands the work of [86] and [87] by including an angiogenic switch characterized by a dynamic tumor carrying capacity that depends on TGF-β secreted by tumor cells. The TGF-β concentration profile follows a Hill function, as was done in [88]. The model includes ordinary differential equations (ODE) describing the change in the concentration of activated (angiogenic) endothelial cells, immunosuppression by Treg cells [89] and TGF-β [90], and the dynamics of additional anti-tumor treatment drugs.

The model simulates the dynamics of wild-type tumor cells T_w that are sensitive to all the simulated treatments, KRAS-mutant cells T_{cp} that are resistant to cetuximab and panitumumab, and irinotecan-resistant cells T_i. The model also includes ODE equations representing the dynamics of NK cells (N), CD8+ T cells (L), Treg cells (R), circulating CD4+ lymphocytes (C), activated endothelial cells (E), IL-2 (I2), TGF-β (B) and the anti-cancer drugs irinotecan (C1), cetuximab and panitumumab (A), sunitinib (S), fresolimumab (F) and a hypothetical chemotherapy drug (C2). The model equations were coded in the open-source numerical computation software Scilab (http://www.scilab.org/) and were solved in Scilab using a built-in 4th-order explicit Runge-Kutta method with fixed step size. This numerical method is efficient, guarantees a stable computation time and has total error $O(h^4)$. Currently, there is not sufficient experimental data to fully parameterize the model with values corresponding to a particular type of cancer. Many parameter values were obtained directly from published models of colorectal cancer, renal cell carcinoma, melanoma and lymphoma. Other parameter values were assumed to be equal to published values for various human cancers.

The following cancer treatments were introduced as inputs to the system to identify the key biological mechanisms and processes that a successful combination therapy should target:

1. chemotherapy (irinotecan) that kills wild-type tumor cells T_w, KRAS-mutant cells T_{cp} and immune cells, but cannot kill irinotecan-resistant cells T_i,
2. a hypothetical chemotherapy drug that does not lead to resistance and can kill wild-type tumor cells Tw and mutant cells (T_{cp} and T_i), but that has the same cytotoxic effects on immune cells as irinotecan chemotherapy. This drug was assumed to have the same dosage, infusion time and injection frequency as irinotecan,
3. two mAbs (cetuximab and panitumumab) that kill wild-type tumor cells T_w directly and enhance tumor cytotoxicity of NK cells, but also lead to increased NK cell death, cannot kill KRAS-mutants T_{cp} directly, and have no chemosensitization effect on irinotecan-resistant cells T_i,
4. a receptor tyrosine kinase inhibitor (sunitinib) that neutralizes the immunosuppressive effect of Treg cells,
5. an anti-angiogenic mAb (fresolimumab) that targets all TGF- β isomers, and
6. adoptive cell transfer of NK cells and CTL.

To generate protocols that are biologically feasible, and that minimize the potential of a patient experiencing life-threatening side effects, published treatment protocols that have been deemed safe were followed. Attention was paid to the safety of the selected dose, frequency, and time required to administer an intravenous injection. For each treatment considered, a positive term representing the rate of drug or cell infusion was introduced in the corresponding ODE to simulate an increase in the concentration of the injected agent in the tumor site.

Equations 1 – 16 define the model of tumor growth that was used to assess the robustness of anti-cancer treatments with respect to the strength of the anti-tumor immune response, with respect to the tumor size at the start of treatment, and with respect to resistance to irinotecan, cetuximab and panitumumab therapies.

$$\begin{aligned}\dot{T}_w &= a_w T_w\left(1-\frac{T_w+T_{cp}+T_i}{T_K+g_2E}\right) - \frac{\mu C_1}{K_M+C_1}T_w \\ &- \left(c+\xi\frac{A}{h_1+A}\right)(e^{-\lambda_T R})NT_w - DT_w \\ &- (K_T+K_{AT}A)\left(\frac{T_w}{\alpha_1 T_{cp}+T_w}\right)(1-e^{-\delta_T(C_1+C_2)})T_w \\ &- \psi A T_w\end{aligned} \tag{1}$$

$$\begin{aligned}\dot{T}_{cp} &= a_m T_{cp}\left(1-\frac{T_w+T_{cp}+T_i}{T_K+g_2E}\right) \\ &- \left(c+\xi\frac{A}{h_1+A}\right)(e^{-\lambda_T R})NT_{cp} \\ &- DT_{cp} - K_T\left(\frac{T_w}{\alpha_1 T_{cp}+T_w}\right)(1-e^{-\delta_{TR}(C_1+C_2)})T_{cp}\end{aligned} \tag{2}$$

$$\dot{T}_i = a_m T_i\left(1-\frac{T_w+T_{cp}+T_i}{T_K+g_2E}\right) + \frac{\mu C_1}{K_M+C_1}T_w - \left(c+\xi\frac{A}{h_1+A}\right)(e^{-\lambda_T R})NT_i - DT_i - (K_T+K_{AT}A)\left(\frac{T_w}{\alpha_1 T_{cp}+T_w}\right)(1-e^{-\delta_{TR}C_2})T_i - \psi A T_i \quad (3)$$

$$\dot{N} = eC - fN - \left(p+p_A\frac{A}{h_1+A}\right)N(T_w+T_{cp}+T_i) + \frac{p_N N I_2}{g_N+I_2} - K_N(1-e^{-\delta_N(C_1+C_2)})N + v_{NK} \quad (4)$$

$$\dot{L} = -\frac{\theta m L}{\theta+I_2} + j\frac{T_w+T_{cp}+T_i}{k+T_w+T_{cp}+T_i}L - qL(T_w+T_{cp}+T_i) + (r_1N+r_2C)(T_w+T_{cp}+T_i) - \frac{uL^2RI_2}{\kappa+I_2} - K_L(1-e^{-\delta_L(C_1+C_2)})L + \frac{p_{I_2}LI_2}{g_{I_2}+I_2} + v_{CTL} \quad (5)$$

$$\dot{C} = \alpha - \beta C - K_C(1-e^{-\delta_C(C_1+C_2)})C \quad (6)$$

$$\dot{E} = b_K E\left(1-\frac{E}{\frac{K_{max}B}{g_1+B}}\right) - d_K E(T_w+T_{cp}+T_i)^{\frac{2}{3}} \quad (7)$$

$$\dot{R} = wC - u_R R + \frac{p_R R I_2}{g_R+I_2} - h_R(1-e^{-\lambda_R S})R - K_R(1-e^{-\delta_R(C_1+C_2)})R \quad (8)$$

$$\dot{C}_1 = -\gamma_1 C_1 + v_{C_1} \quad (9)$$

$$\dot{C}_2 = -\gamma_2 C_2 + v_{C_2} \quad (10)$$

$$\dot{I}_2 = -\mu_{I_2} I_2 + \phi C + \frac{\omega L I_2}{\varsigma+I_2} + v_{I_2} \quad (11)$$

$$\dot{A} = -\eta A - \lambda(T_w+T_{cp}+T_i)\left(\frac{A}{h_2+A}\right) + v_A \quad (12)$$

$$\dot{B} = p_1\frac{(T_w+T_{cp}+T_i)^2}{b_1^2+(T_w+T_{cp}+T_i)^2} - u_1 B - b_2 F B \quad (13)$$

$$\dot{S} = -\eta_S S + v_S \quad (14)$$

$$\dot{F} = -\eta_F F - b_3 B F + v_F \quad (15)$$

Equation 16 below was defined in [91] to set the level of strength of the anti-tumor immune response. It was expanded by [87] to consider the presence of KRAS mutant tumor cells. We expanded it further to include irinotecan-resistant cells and the immunosuppressive effect of TGF-β on the tumor cell killing rate *d* by CD8+ T cells.

$$D = \left(\frac{d}{1+B/S_1}\right)\cdot\frac{\left(\frac{L}{T_w+T_{cp}+T_i}\right)^l}{s+\left(\frac{L}{T_w+T_{cp}+T_i}\right)^l} \quad (16)$$

The definition of the model variables, their units and their initial values are listed in Table 1. These initial conditions are similar to those in [87]. Since the initial tumor size used in all the simulations was well above the diffusion-limited value of 10^6 cells, it was assumed that the tumor was already well vascularized. This is reflected by the high concentration of TGF-β and activated endothelial cells prior to the start of treatment. Moreover, a large tumor creates a highly immunosuppressive microenvironment. This high immunosuppressive state was simulated by assuming a high initial concentration of regulatory T cells in all the simulations.

Table 2 lists all the treatments that were simulated, including a description of the dose, frequency and the time required for administration. ODEs were used to simulate all treatments as intravenous injections of constant infusion rate, except sunitinib, which is given orally. The infusion rate terms that appear in the ODEs and that are listed in the rightmost column of Table 2 were obtained by assuming, as was done in [86], that an adult has an average weight of 70 kg, an average surface area of 1.73 m^2 and an average body volume of 59.71 liters. A more detailed explanation of how the infusion rates of irinotecan, cetixumab and patinumumab were computed can be found in [86].

Supplementary Table 1 in the Appendix lists the parameter values that were used in the simulations. Some parameter values are different for cetuximab and panitumumab due to their mechanism of action and their effect, or lack thereof, on tumor growth. The parameter values that the authors estimated were chosen based on assumed similarities between two processes or between cytokines that exert similar functions. For example, the suppressive effect of Treg cells on the wild-type tumor cell kill rate by NK cells was assumed to be the same as the suppressive effect of Tregs on mutant tumor cell kill rate by NK cells, the growth rate of mutant tumor cells was assumed to be the same as that of wild-type tumor cells, and the degradation rate of anti-TGF-® was assumed to be the same as that of anti-VEGF. Since the model parameterization is based on process rates corresponding to

distinct cancer types that were obtained from *in vitro* experiments, the model dynamics and predictions should be interpreted as a generalization of cancer dynamics and potential treatment outcomes. The experimental and computational methods used to obtain many of the parameter values are described in [86, 89]. Whenever necessary, the concentration units of TGF-® and anti-TGF-® were converted from mg/L to IU/L, and vice versa, by referring to the published specific activity of TGF-®. An example of how to perform this conversion can be found in [94].

The parameters *d*, *l* and *s* together determine the level of strength of a patient's immune system response *D*, as defined by equation 15. The values of these parameters are taken from the sets $d \in \{1.3, 1.6, 2.1\}$, $l \in \{2, 1.1, 1.4\}$ and $s \in \{0.04, 0.008, 0.005\}$. A strong immune response (D_s) corresponds to the combination of values $(d = 2.1, l = 1.1, s = 0.005)$, a moderate response ($D_m$) corresponds to the values $(d = 1.6, l = 1.4, s = 0.008)$, and a weak response ($D_w$) is characterized by the values $(d = 1.3, l = 2, s = 0.04)$. These levels of immune strength are the same as those that were considered in [86].

The anti-cancer treatments listed in Table 2, as well as certain combinations of them, were assessed for their robustness with respect to the three levels of immune strength D_s, D_m, and D_w. To assess the robustness of a treatment with respect to tumor size, initial tumor sizes of up to 10^9 cells were considered. Robustness with respect to resistance to therapy was assessed by comparing two cases: 1) a case where wild-type tumor cells cannot become resistant to any treatment and there are no mutant cells present at the start of treatment, and 2) a case where there are 35 KRAS-mutant tumor cells initially present, and there are no irinotecan-resistant cells present, but irinotecan resistance emerges in an irinotecan dose-dependent manner. The emergence of irinotecan resistance is represented by the term

$$\frac{\mu T_w C_1}{K_M + C_1}$$

that appears in equations 1 and 3.

Cancer therapy tends to have side effects that must be kept into consideration when designing a treatment protocol. Chemotherapy has the undesirable effect of killing a significant number of immune cells. Cetuximab and panitumumab lead to NK cell death due to their interaction with mAb-tumor complexes. To ensure the safety in the clinic of all the simulated treatments that led to a significant reduction in tumor size, the criteria for minimum circulating lymphocyte concentration of 1.4×10^8 lymphocytes per liter set by the World Health Organization (WHO) [95] was enforced. Depending on the effectiveness of a particular treatment, the predicted outcome was the elimination of the tumor, reduced or arrested growth, or continued growth. In all the simulations, a complete response (CR) to a cancer treatment was defined as a tumor size at the end of the treatment period that is less than or equal to the diffusion-limited value of 1×10^6 tumor cells. Hence, a complete response is characterized by a reduction in tumor size below the threshold that would trigger the angiogenic switch. A partial response (PR) to treatment is described by a tumor that remains larger than 1×10^6 cells, but that by the end of the treatment period is smaller than at the start of treatment. The no response (NR) classification applies when tumor size remains the same, or becomes larger than it was at the start of treatment, by the time the treatment period ends.

Table 1. Model Variables and their Initial Values

Variable	Definition	Units	Initial Value
T_w	Number of wild-type cancer cells sensitive to cetuximab, panitumumab and irinotecan	cells	1×10^9
T_{cp}	Number of mutant cancer cells resistant to cetuximab and panitumumab and that are sensitive to irinotecan and the hypothetical chemotherapy drug C_2	cells	35
T_i	Number of mutant cancer cells resistant to irinotecan and that are sensitive to cetuximab, panitumumab and the hypothetical chemotherapy drug C_2	cells	0
N	Concentration of NK cells per liter of blood	cells / L	9×10^7
L	Concentration of CD8+ T cells per liter of blood	cells / L	1.8×10^5
C	Concentration per liter of blood of other circulating lymphocytes not including NK cells, CD8+ T cells or regulatory T cells	cells / L	9×10^8
E	Number of activated endothelial cells	cells	2×10^9
R	Concentration of regulatory T cells per liter of blood	cells / L	4×10^8
C_1	Concentration of the chemotherapy agent irinotecan per liter of blood	mg / L	0
C_2	Concentration of a hypothetical chemotherapy agent per liter of blood	mg / L	0
I_2	Concentration of IL-2 per liter of blood	IU / L	1173
A	Concentration of the monoclonal antibodies cetuximab and panitumumab per liter of blood	mg / L	0
B	Concentration of TGF-® per liter of blood	IU / L	1×10^4
S	Concentration of the tyrosine kinase inhibitor sunitinib per liter of blood	mg / L	0
F	Concentration of the monoclonal antibody fresolimumab per liter of blood	mg / L	0

Table 2. Treatment Dose and Frequency

Treatment Modality	Agent / Cell Type	Dose and Frequency	Infusion Time	Infusion Rate
Chemotherapy	Irinotecan [86]	125 mg/m^2 given weekly. This cycle may be repeated.	1.5 hr	$v_{C_1} = 57.947 \ \frac{mg}{L \cdot day}$
Chemotherapy	(Hypothetical)	125 mg/m^2 given weekly. This chemotherapy agent was assumed to have the same cytotoxic properties on the tumor and immune cells as irinotecan. It was assumed that tumor cells never develop resistance to this drug. This cycle may be repeated.	1.5 hr	$v_{C_2} = 57.947 \ \frac{mg}{L \cdot day}$
Monoclonal antibody	Cetuximab [86]	Loading dose (LD): 400 mg/m^2 (a one-time injection before giving the maintenance doses) Maintenance dose (MD): 250 mg/m^2 (given weekly – start one week after giving LD and rest 2 weeks every 4 weeks). This cycle may be repeated.	LD: 2 hr MD: 1 hr	$LD: v_A = 139.072 \ \frac{mg}{L \cdot day}$ $MD: v_A = 173.840 \ \frac{mg}{L \cdot day}$ Note: the same infusion term v_A is used for cetuximab and for panitumumab, but their v_A values are different.
Monoclonal antibody	Panitumumab [86]	6 mg/kg every two weeks. No loading dose is required. This cycle may be repeated.	1 hr	$v_A = 168.816 \ \frac{mg}{L \cdot day}$
Monoclonal antibody	Fresolimumab [20]	3 mg/kg every two weeks. This cycle may be repeated.	1.5 hr	$v_F = 56.272 \ \frac{mg}{L \cdot day}$
RTK inhibitor	Sunitinib [89]	A sunitinib capsule is given daily for 28 straight days followed by two weeks of rest. In total, 23.447 mg of sunitinib are administered per each 6-week cycle. This cycle may be repeated.	None	$v_S = 0.8374 \ \frac{mg}{L \cdot day}$
Adoptive cell transfer	NK cells [92]	An intravenous injection of 2×10^7 NK cells per kg is given weekly. This cycle may be repeated.	1 hr	$v_{NK} = 5.627\times10^8 \ \frac{cells}{L \cdot day}$
Adoptive cell transfer	CTL [93]	Five intravenous injections of 1×10^{10} CTL per m^2 are given every 5 days and they are followed by 45 days of rest. This 65-day cycle may be repeated.	1 hr	$v_{CTL} = 6.9536\times10^9 \ \frac{cells}{L \cdot day}$
Cytokine Treatment	IL-2 [48]	180,000 IU/kg injected over 15 minutes every 8 hours. Twenty-one injections were given. IL-2 injections had no significant effect on tumor growth when given as monotherapy or in combination with other treatments.	0.25 hr	$v_{IL_2} = 2.0258\times10^7 \ \frac{IU}{L \cdot day}$

A cancer treatment that leads to a complete response (CR) at the three levels of immune response strength *D*, for tumor sizes of up to 10^9 cells at the start of treatment, does not lead to the emergence of treatment resistance and is effective in spite of resistant cells being present, and that meets the minimum lymphocyte concentration criteria for safety of at least 1.4×10^8 circulating lymphocytes per liter throughout the treatment period, is defined as being *robust with respect to the above perturbations*. This is the definition of robustness of an anti-cancer treatment that was considered in the computational analysis presented in the next section.

3. Results

The results presented in Section 3.1.1 show that without angiogenesis and no immune system action, the tumor remains avascular and can only grow to its diffusion-limited size of 1 million cells. Through secretion of TGF-β that activates endothelial cells, tumor cells elicit angiogenesis, which increases the carrying capacity of the tumor. Section 3.1.2 discusses the predicted tumor growth with angiogenesis for three distinct levels of immune response strength for initial tumor sizes up to 10^9 cells. The simulations predict that if the tumor is smaller than a *therapeutic size threshold* that depends on the level of immune strength, the immune system alone will be able to eliminate the tumor. The robustness, or lack thereof, of various anti-cancer treatments is discussed in Section 3.2, with the assumption that wild-type tumor cells never mutate to become resistant to therapy and that there are no mutant tumor cells present before treatment begins. Section 3.3 describes a combination therapy that was found to be robust with respect to immune system strength, initial tumor size and treatment resistance. Lastly, Section 3.4 presents the results of the sensitivity analysis that was performed on the model parameters.

3.1. No Treatment Administration

3.1.1. No Immune System Action

Figure 1A shows that in the absence of an active immune system and no anti-cancer treatment, a tumor that is unable to undergo an angiogenic switch will remain at the diffusion-limited size of 1 million cells. A tumor with an initial size of less than a million cells will not grow beyond this asymptotic size and will remain avascular, posing little risk of metastasis. Figure 1B shows that a tumor that is larger than 1 million cells will shrink the diffusion-limited size due to cell death, if it is unable to release cytokines that activate endothelial cells to start the process of angiogenesis.

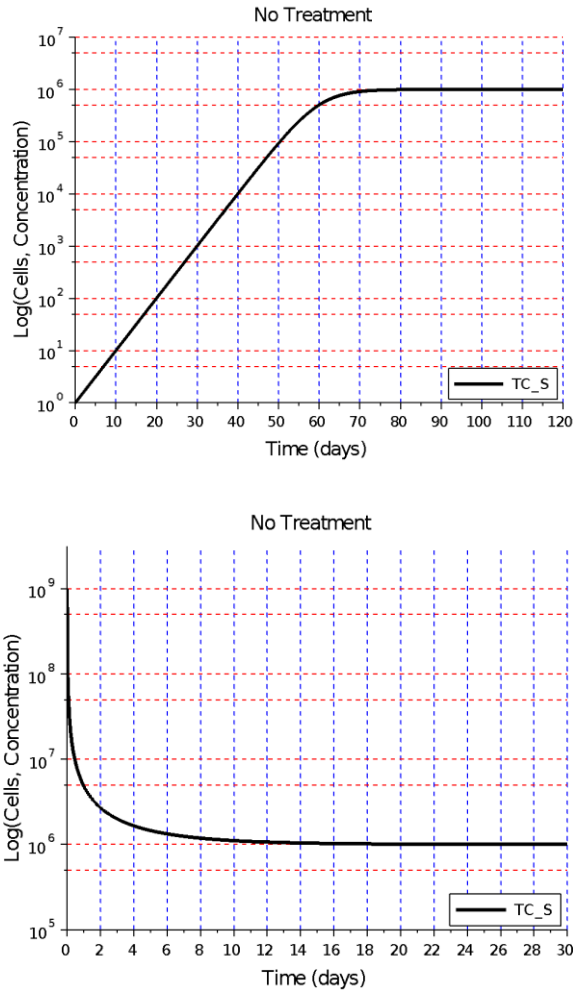

Figure 1. Tumor growth without angiogenesis and no immune system action. A) In the absence of angiogenesis, no immune system action, and no treatment, a small tumor is able to grow up to the diffusion-limited size of 1 million cells. B) A tumor larger than 1 million cells will shrink to the diffusion-limited size due to cell death cause by an insufficient flow of nutrients into the tumor

Figure 2 shows that a small tumor that undergoes an angiogenic switch via TGF-β (or VEGF) secretion will attain a size much larger than the diffusion-limited size. The maximum tumor size that can be attained depends on the extent of endothelial cell activation and how well this activation leads to vasculature formation and maturation. In the model, the maximum carrying capacity of activated endothelial cells was assumed to be 5×10^9 EC. It was also assumed that each endothelial cell that becomes activated increases the tumor carrying capacity by 1 tumor cell. Hence, an angiogenic switch allows a simulated tumor to increase its carrying capacity by up to 5×10^9 tumor cells.

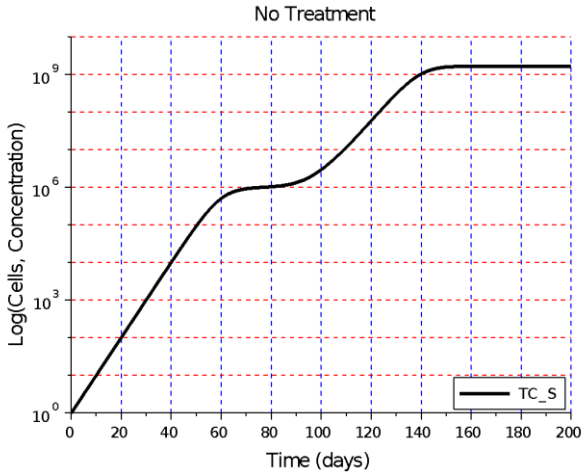

Figure 2. Hypothetical angiogenic switch driven by TGF-β secretion. In this simulation, undergoing an angiogenic switch allowed the tumor to attain the asymptotic size of 1.6275×10^9 cells on day 200. The figure illustrates a tumor dormancy of approximately one week. The dormancy period may be longer or may be nonexistent, depending on the environmental conditions and the type of tumor

Once a tumor has undergone an angiogenic switch due to increased hypoxic conditions, it releases angiogenic cytokines at a greater rate that allows the tumor to increase its rate of growth and attain a much larger size. Since angiogenic cytokines such as TGF-β and VEGF are also immunosuppressive, it becomes more and more difficult for the immune system to destroy a solid tumor as it continues to grow. Eventually, a large tumor may be able to suppress the anti-tumor immune response sufficiently to escape destruction. Due to the dual role of TGF-β and VEGF as stimulators of tumor angiogenesis and as immunosuppressors, these cytokines are important treatment targets.

3.1.2. Immune System Action

The effect of the immune system on the growth of an angiogenic tumor depends on the antigenicity of the tumor and the strength of the immune response. The model simulations show that for each level of immune strength there exists a therapeutic tumor size threshold value below which an immune system of a particular strength will be able to eliminate the tumor. Figure 3A shows the effect of a strong immune response D_s on tumor growth in the presence of immunosuppression and the absence of treatment. In this case, a tumor of size up to 1×10^8 cells will be eliminated without the need for treatment. This

outcome represents the ideal case, where a body's own defenses eliminate an infection without the need for medical intervention. The decrease in the number of activated endothelial cells (EC), shown in all the figures as a thick black line, is due to a decrease in TGF-β secreted by tumor cells. As immune cells continue to kill tumor cells, the concentration of TGF-β decreases, leading to endothelial cell deactivation and a decrease in the carrying capacity of activated ECs and of tumor cells. The thin black line represents the actual number of tumor cells over time.

The therapeutic tumor size threshold corresponding to a moderate strength D_m is predicted to be approximately 1×10^7 cells. Figure 3B shows that if a tumor has a size that is above this threshold, a compromised immune system capable of only a moderate anti-tumor response will not be able to arrest tumor growth. The tumor will eventually attain a size equal to its dynamic carrying capacity. This escape from immunodestruction by the tumor is due to a tip of the balance between the strength of the anti-tumor immune response and immunosuppression exerted by Treg cells in favor of immunosuppression. Figure 3C illustrates the prediction that if the immune response is weak (D_w), only tumors that have a size equal to or smaller than the diffusion-limited size of 1 million cells will be destroyed by the immune system. Hence, in the absence of treatment, an immune system that exhibits a weak anti-tumor response can only eliminate avascular tumors.

An important aspect that is worth emphasizing is the fact that, since no treatment was administered in any of the cases discussed so far, the concentration of lymphocytes remained approximately the same. However, as we will see in the next section, chemotherapy and certain monoclonal antibody therapies (e.g. cetuximab and panitumumab) exhibit a cytotoxicity that kills tumor cells as well as lymphocytes such as NK cells and CD8+ T cells. This places a restriction on the dose and frequency of these types of treatments. Treatment safety with respect to the number of circulating lymphocytes during the period of treatment was taken into consideration in all the simulations that are presented in Sections 3.2 and 3.3.

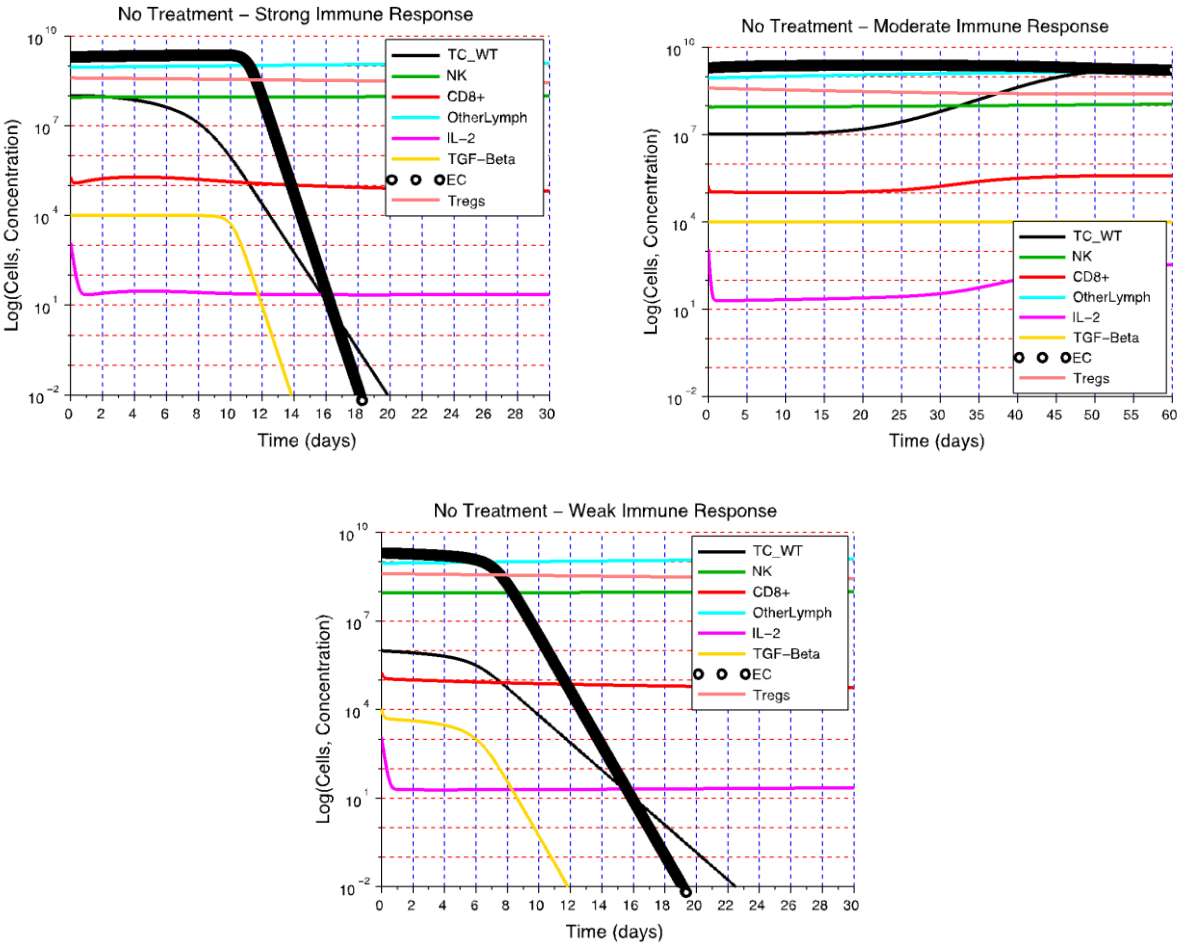

Figure 3. Tumor growth for different levels of immune strength D without treatment. A) In the presence of immunosuppression and the absence of treatment, a strong immune response D_s is able to eliminate a tumor consisting of up to 1×10^8 cells. B) Without treatment, a moderate immune response D_m is not able to eliminate a tumor that is larger than 1×10^7 cells. C) If the immune response is weak (D_w), only non-vascularized tumors consisting of less than 1 million cells will be eliminated in the absence of treatment

3.2. Treatment Administration without Resistance

3.2.1. No Immune System Action

The potential of a treatment to eradicate a tumor in the absence of an immune response, and without resistance to treatment was investigated next. To simulate this scenario, the anti-tumor effect of NK cells, CD8+ T cells and circulating lymphocytes, the immunosuppressive activity of Treg cells and the mutation rate of wild-type tumor cells were all turned off. However, the potential of a tumor to undergo an angiogenic switch through release of TGF-β, resulting in activation of endothelial cells, was left intact. To eliminate the case of KRAS-mutants being present at the start of treatment, the initial number of KRAS-mutants was set to zero. To exclude the dose-dependent emergence of irinotecan-resistant cells, the parameter μ was set to zero. Initial tumor sizes up to 10^9 cells were considered. None of the monotherapies listed in Table 2, or their combinations, led to a complete response (CR) or a partial response (PR) when an anti-tumor immune response was absent. These results hint at the important role of the immune system in helping to destroy cancer cells that remain after a first-line therapy decreases tumor size below the corresponding therapeutic threshold. A natural anti-tumor immune response obviates the need to increase the dose or frequency of a first-line therapy, reducing the potential of harmful side effects that could result if a treatment were to be given for an extended period of time.

3.2.2. Immune System Action

To assess the robustness of a treatment with respect to the level of immune strength and the size of the tumor at the start of the treatment, the best-case scenario for tumor treatment was first considered: a strong immune response D_s. The combination therapies that were simulated using the model are listed in Supplementary Table 2 in the Appendix. The only protocol that met the criteria for robustness and that was classified as being robust with respect to the level of immune strength and initial tumor size was the sunitinib + fresolimumab combination therapy. Sunitinib reduces immunosuppression by reducing the concentration of Treg cells in patients, while fresolimumab blocks the angiogenic effect of TGF-β, thus reducing the dynamic carrying capacity of tumor cells. Based on model simulations, these two drugs were ineffective in reducing tumor growth when given as monotherapy if the strength of the immune response was weak. On the other hand, giving these two treatments concurrently led to a synergy that made this combination treatment robust with respect to the three levels of D and with respect to tumor size at the start of treatment. Figure 4 illustrates the failure of sunitinib and fresolimumab monotherapies and the success of sunitinib + fresolimumab combination therapy for immune response strength D_w with an initial tumor size of 10^9 cells.

When sunitinib is given as monotherapy in a clinical setting, patients undergo an average of 5 cycles of sunitinib capsule intake (28 capsules per cycle). The therapeutic effect of combination therapy illustrated in Figure 4C suggests that at most two cycles of sunitinib may be necessary to eliminate the tumor when combined with 3 biweekly injections of fresolimumab. This particular combinatorial approach to treat cancer has the potential to reduce the cost of treatment and is safe, since neither drug has a cytotoxic effect on immune cells. This is in contrast to chemotherapy, which tends to kill CD8+ T cells and NK cells.

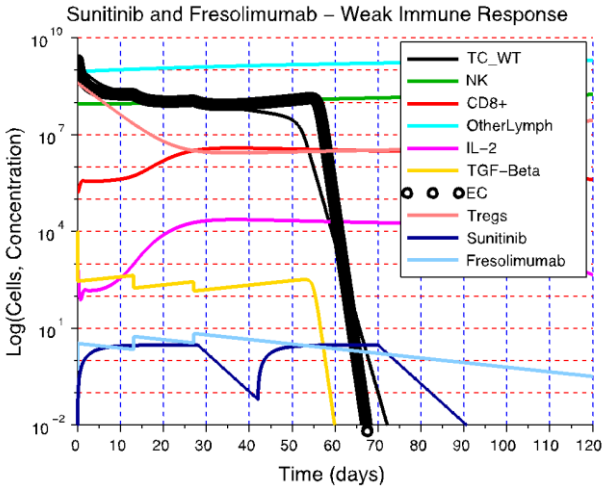

Figure 4. A synergistic effect of sunitinib and fresolimumab leads to robustness with respect to immune strength D and to initial tumor size. A) The immune strength is so weak that a significant reduction of Treg cell concentration is not sufficient to boost the immune response enough to be able to take over and eliminate the tumor. B) By neutralizing TGF-β and reducing its concentration, fresolimumab monotherapy reduces tumor size below the initial size of 10^9 cells. However, the immune strength is weak and the concentration of Treg cells is high. In this case, it is not possible for the immune system to capitalize on the reduction in tumor size achieved through administration of fresolimumab. C) A reduction in tumor size by fresolimumab, combined with a decrease in the immunosuppressive effect of Treg cells due to sunitinib action, leads to synergy and complete tumor destruction even when the anti-tumor immune strength is weak

The sunitinib + fresolimumab combination therapy was the only protocol that exhibited robustness to changes in immune response strength D and initial tumor size. A treatment that is robust with respect to D is an ideal treatment because it will be beneficial to a larger number of patients whose immune response strength varies from patient to patient, or varies during the period of treatment. However, the model also predicts that treatment robustness is not required for treatment success *at a particular D level* if two or more distinct treatment modalities synergize at that level of immune response. Some combination therapies were identified that, although they are not robust with respect to immune response strength, they showed a synergistic effect at a particular D level that could be effective in a clinical setting. For example, the model predicted that neither NK cell monotherapy, CTL monotherapy nor irinotecan chemotherapy can lead to tumor eradication at the D_m level. However, when an NK

cell or CTL treatment was combined with first-line irinotecan monotherapy, the resulting combination therapy eliminated tumors consisting of as may as 10^9 cells at the moderate immune response level D_m or higher.

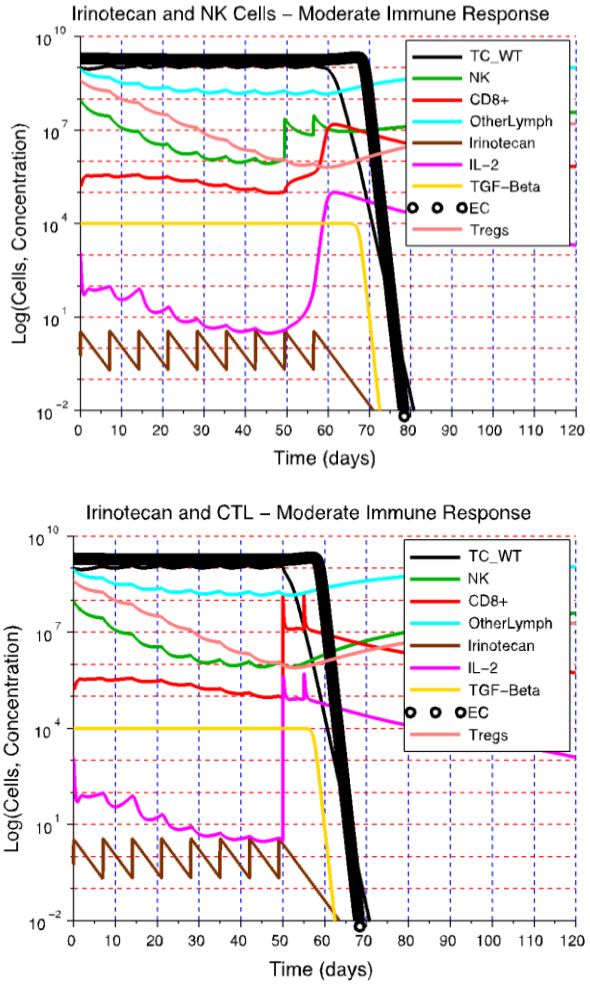

Figure 5. Tumor elimination through an I+NK cell treatment and an I+CTL treatment at the D_m immune response level. A) A weekly NK cell treatment started on day 49 restores the NK cell activity that had been attenuated by chemotherapy. A high NK cell concentration together with a low Treg cell concentration leads to tumor eradication. B) Irinotecan chemotherapy reduces immunosuppression to a point that CTL therapy is successful if it is started after day 50. In I+CTL treatment, the concentration of CTL increases significantly after CTL injections are given, while the concentrations of NK cells and Treg cells remain low. The strong CTL activity eliminates the tumor in spite of the decrease in NK cell activity caused by the chemotherapy. The default parameter values for cetuximab were used to simulate the I+NK cell and I+CTL therapies

The irinotecan + NK (I+NK) combination treatment consisted of giving a total of 9 weekly irinotecan injections and 2 concurrent weekly NK cell injections starting with the 8^{th} irinotecan injection. The recommendation of not giving the NK cell treatment earlier is based on Figure 5A, which shows that it takes about 7 weeks of irinotecan chemotherapy for Treg cell concentration to decrease substantially, which decreases immunosuppression significantly. The effectiveness of the injected NK cells in killing the remaining tumor cells is maximized if they are injected after 8 weeks of chemotherapy. After day 55 the concentration of CD8+ T cells rose to be an order of magnitude greater than that of Treg cells, which contributed to the success of the NK cells that were injected starting on day 49.

Figure 5B shows an example of an irinotecan + CTL (I+CTL) combination therapy that, although not robust with respect to the level of the immune response, is effective in eliminating the tumor when the immune response is moderate. In the I+CTL treatment, 8 irinotecan injections were administered in total. Two CTL injections were given, starting on day 50, when Treg cell concentration approached its lowest value. The infusion of CTL on day 50 resulted in a drastic increase in CTL concentration, such that CTL concentration became significantly higher than Treg cell concentration. The appropriate timing of CTL injections combined with the first-line irinotecan chemotherapy tipped the balance between anti-tumor immune activity and immunosuppression in favor of the former, leading to synergy between these two modalities that resulted in tumor elimination.

The results presented in Figure 5 are relevant because they indicate that patients whose immune system has been compromised to the point of exhibiting only a moderate immune response could still benefit from an I+NK or I+CTL combination therapy. The I+NK and I+CTL simulations illustrate the importance of injection timing to achieve synergy. A high NK cell or CTL concentration coupled with a simultaneously low Treg concentration is what tipped the balance in favor of the anti-tumor immune response and led to the elimination of the tumor. The synergy between the co-treatments also reduced the total number of required injections. The model predicts that infusing NK cells or CTL cells during the first few weeks after starting the chemotherapy will not lead to tumor eradication due to the high concentration of Treg cells at this phase of the treatment, which would attenuate the cytotoxic effect on tumor cells of the infused NK cells or CTL cells.

3.3. Treatment Resistance

The presence or emergence of mutant cells resistant to cetuximab, panitumumab or irinotecan may explain why combination treatments that involve these drugs fail to eliminate a tumor in a clinical setting. In the irinotecan + panitumumab combination therapy shown in Figure 6, irinotecan is given weekly and panitumumab biweekly. Continuing to give this combination treatment for several months leads to the elimination of irinotecan-resistant cells through the action of panitimumab, while the wild-type cells are eliminated by the enhanced cytotoxic effect of irinotecan + panitumumab. However, the KRAS mutants ultimately survive because they do not experience the enhanced cytotoxic effect of irinotecan + panitumumab. At steady state, the tumor will consist of approximately 1.63×10^9 panitumumab-resistant cells, leading to treatment failure.

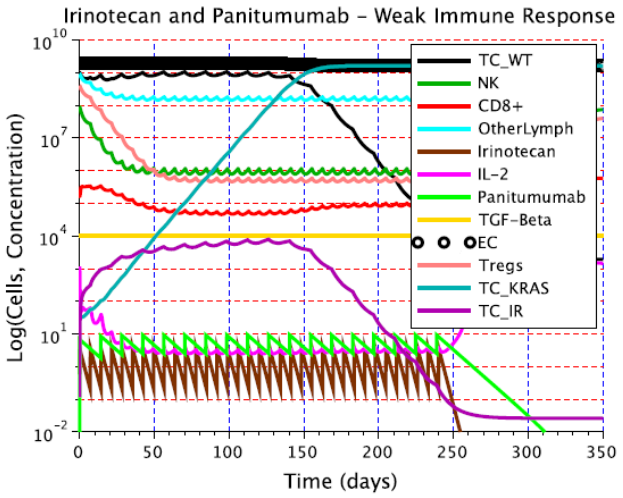

Figure 6. The emergence of resistance to irinotecan + panitumumab combination therapy. This combination therapy is unable to kill the KRAS mutants, which are resistant to panitumumab. Consequently, the KRAS mutants continue to grow to their carrying capacity. This simulation assumed a weak immune response D_w, and an initial population of 10^9 wild-type tumor cells. The parameter values corresponding to panitumumab were used in this simulation

The irinotecan + panitumumab treatment simulation is an example of a combination therapy that fails to eliminate a tumor that contains KRAS-mutant cells. The simulations also show that a combination of irinotecan and panitumumab (or a combination of irinotecan + cetuximab) leads to a greater NK cell death, making it difficult to boost the immune system if NK cells were to be injected while both irinotecan and panitumumab injections continue to be administered. This example makes it evident that not all combination therapies are necessarily more effective than a monotherapy in reducing tumor size. For combination therapy to be useful, it is important to understand the effect that each drug has on the tumor cells as well as on the immune cells, and how to modulate the dose and frequency of each mode to maximize the combined therapeutic effect without cancelling or attenuating the action of one of the co-treatments.

The model was able to replicate the results of Sameen et al. [87] that irinotecan + cetuximab and irinotecan + panitimumab combination therapies are effective in eliminating a tumor only in a patient whose anti-tumor immune response is strong. Since such a strong immune response is not common among cancer patients, the model in [87] and our model both suggest that this type of combination therapy should not be given as a first-line treatment. If either irinotecan + cetuximab or irinotecan + panitimumab is given, this combination therapy should be supplemented with a different treatment modality that will be able to eliminate the KRAS mutant cells and irinotican resistant cells that may arise during the treatment phase.

In order to assess treatment robustness with respect to present and emergent resistance, the following categories were established:

1. The treatment is robust with respect to all levels of immune strength D, the tumor size at the start of treatment, and with respect to the emergence of resistance. This treatment does not lead to the transformation of wild-type cancer cells into mutant cells, and results in a complete response (CR) at all levels of D and initial tumor size up to 10^9 cells. If irinotecan-resistant cells and/or KRAS mutants are already present, the treatment still leads to a CR.
2. The treatment is robust with respect to the emergence of resistance and leads to a complete response (CR) for an initial tumor size up to 10^9 cells at the strong and moderate immune strength levels only.

Table 3 lists the combination therapies that were classified as belonging to category 1 or to category 2. The list in category 2 is only partial. Other treatments that are not robust with respect to the level of immune response strength, but that are robust at the D_m level with respect to initial tumor size at the start of treatment and with respect to treatment resistance, are listed in Supplementary Table 2.

Table 3 shows that only a sunitinib + fresolimumab combination treatment exhibited robustness in producing a complete response with respect to all the perturbations that were considered. The model predicted that a sunitinib + fresolimumab protocol has the potential to eliminate, in a relatively short time, a large, heterogeneous tumor consisting of wild-type and mutant cells in a patient whose anti-tumor immune response is moderate or weak. Unfortunately, treatment robustness may not be easy to achieve in practice. A robust cancer treatment requires combining modalities that can lead to strong synergy, but strong synergy can only be achieved if the correct dose, timing and frequency are implemented. The model helped to determine on what day to start a particular type of treatment to achieve the strongest synergy possible. Mathematical modeling that drives experimentation can provide the guidance necessary to identify a protocol that can be made robust with respect to changes in tumor characteristics and changes in a patient's immune activity profile.

The simulations indicated that for protocols that were not robust with respect to the strength of the immune response, but that eliminated a heterogeneous tumor consisting of up to 10^9 wild-type and mutant cells at a moderate immune response strength, the key ingredient was a timely adoptive cell transfer. For example, in the successful non-robust combination treatments F+NK, I+NK, I+CTL, and S+P+NK, it was the injected NK or CTL cells that provided the necessary boost at the right time to the patient's immune system to tip the balance in favor of immunodestruction of the tumor. The model predicts that in order to increase the likelihood of treatment success, immunosuppression must be reduced significantly prior to starting ACT, and a patient's immune system must be capable of at least a moderate anti-tumor response.

Table 3. Description of Robust and Effective Treatments

Category	Treatment Components	Description of the Treatment
1 (Robust)	Sunitinib + Fresolimumab (S+F)	Give one cycle of daily sunitinib capsules (28 capsules in total the first 4 weeks, followed by two weeks of rest, and then stop sunitinib treatment), while concurrently giving 2 biweekly injections of fresolimumab starting on day 0. **Comments:** This combination therapy requires a small number of fresolimumab injections to achieve a CR, which significantly reduces the side effects associated with anti-TGF-β therapies. This combination therapy did not lead to treatment resistance and eliminated wild-type, irinotecan-resistant and KRAS-mutant tumor cells that were already present. It takes about 37 days to achieve a CR, which is one of the shortest times to eradication compared to the successful but non-robust treatments in Category 2.
2 (Not Robust but Effective in Achieving a CR)	Fresolimumab Monotherapy (F)	Give 10 biweekly injections of fresolimumab. **Comments:** This successful monotherapy required at least 10 biweekly injections to achieve CR. The model predicts tumor elimination on day 157 (about 5 months after the start of treatment). The disadvantages of this long period of treatment are cost, and an increased risk of harmful side effects that may require temporary or permanent discontinuation of the treatment.
	Fresolimumab + NK Cells (F+NK)	Give 7 biweekly injections of fresolimumab. Concurrently, give 14 weekly injections of NK cells starting on day 0. **Comments:** Neither fresolimumab nor NK cell monotherapies or combined therapy lead to the development of mutant cancer cells. Fresolimumab decreases tumor size over time by neutralizing TGF-β, while NK cell injections increase NK cell concentration. However, none of these treatments decrease the immunosuppressive effect of Treg cells. Consequently, it is not until the NK cell concentration has increased substantially that the immune system is able to take over and eliminate the tumor. Although it takes about 103 days to achieve a CR with this combination therapy, this time to tumor eradication is considerably shorter than the 157 days that would take to achieve a CR when fresolimumab is given as monotherapy.
	Irinotecan + NK cells (I+NK)	Give 10 weekly irinotecan injections and concurrently give 3 weekly NK cell injections starting at the time when the 8th irinotecan injection is given. **Comments:** The model predicts that irinotecan chemotherapy will lead to the emergence of irinotecan-resistant cancer cells. The wild-type and resistant populations will continue to grow over time, while Treg cell concentration will decrease steadily by 3 orders of magnitude. It is at this point that the 3 NK cell injections can be administered to eliminate the chemosensitive and resistant cells. It takes about 80 days to achieve a CR.
	Irinotecan + CTL (I+CTL)	Give 11 weekly irinotecan injections and concurrently give 5 CTL injections (one CTL injection every 5 days) starting on day 60 after 9 irinotecan injections have been given. **Comments:** At first, irinotecan chemotherapy will lead to the emergence of resistant cells. The wild-type and resistant populations will continue to grow over time, while Treg cell concentration will decreases by over 2 orders of magnitude. Once Treg cell concentration stabilizes at a minimum value, the CTL treatment can be started to eliminate all the sensitive and resistant tumor cells. It takes about 81 days to achieve a CR.
	Sunitinib + Panitumumab + NK Cells (S+P+NK)	Give 2 cycles of sunitinib capsules as first-line treatment concurrently with 6 biweekly panitumumab injections. Also, give 4 weekly NK cell injections starting on the same day when the 4th panitumumab injection is given. **Comments:** Sunitinib reduces Treg cell concentration by slightly more than 2 orders of magnitude while panitumumab is able to decrease tumor size slightly. However, due to the moderate level of immune response, the tumor starts to grow back up during the two weeks between panitumumab injections. The timely boost of anti-tumor immune system activity that eliminates the tumor is achieved by the 4 NK cell injections that are given when Treg cell concentration is low enough. Both wild-type and KRAS mutant cells are eliminated by the infused NK cells. It takes about 90 days to achieve a CR.

A successful immune response depends on the cooperation of multiple immune cells. Boosting the anti-tumor activity of only one immune cell type may not be sufficient to guarantee tumor growth arrest if the anti-tumor immune response of a patient is weak. When the anti-tumor response of a key component of the immune system is not working optimally, such as CD8+ T cells, tumor elimination may not be possible after adoptive cell transfer of NK cells, even if immunosuppression is reduced by the treatment. An example of this phenomenon occurs during the administration of Sunitinib + Panitumumab + NK cell combination therapy if a patient has an immune system that exhibits a weak response. The unsuccessful outcome of this treatment is illustrated in Figure 7A.

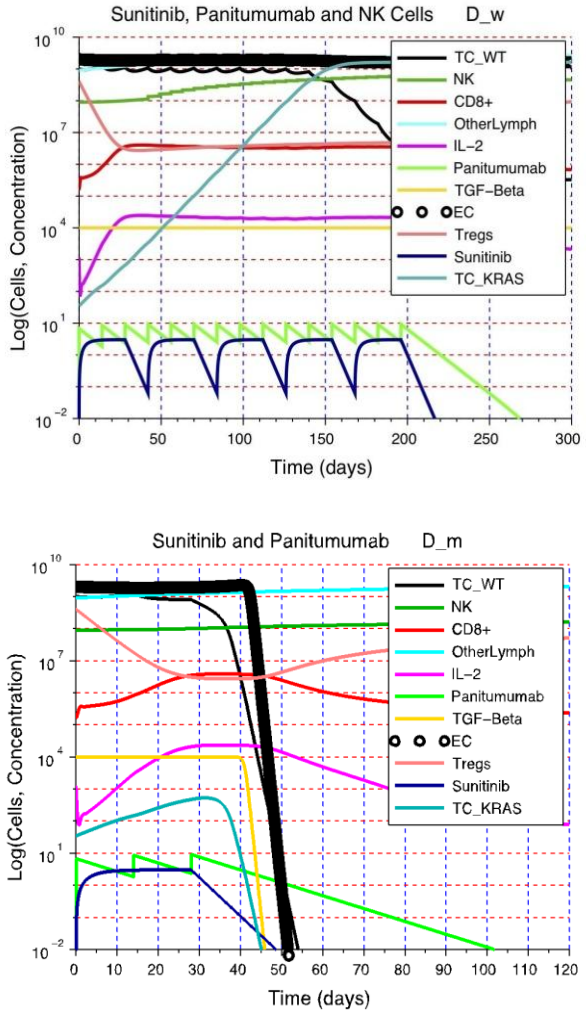

Figure 7. The importance of the immune response strength *D* on treatment outcome. A) Although NK cell activity increases after the adoptive cell transfer, while immunosuppression is decreased by the sunitinib injections, these simultaneous changes in immunosuppression and NK cell activity are not sufficient to eliminate the tumor. The end result is a heterogeneous tumor consisting of wild-type tumor cells and KRAS mutants that is more difficult to treat. This example illustrates the need to design patient-specific treatments that take into account, and can address, the deficiencies in a patient's immune system status. B) A patient with an immune system capable of a moderate response can benefit from a single cycle of sunitinib + panitumumab. The wild-type and KRAS mutant tumor cells are eliminated due to the moderate strength of the anti-tumor response combined with the synergistic effect of sunitinib + panitumumab

The model simulations for cetuximab and panitumumab treatments predict that a strong immune system can counteract the presence of KRAS-mutant tumor cells as well as the emergence of irinotecan-resistant cells. This is to be expected, since both of these types of mutant cells remain vulnerable to immune destruction if their antigenicity is sufficiently high and the immune system is capable of a strong response. Figure 8 illustrates the elimination of wild-type and mutant cells due to a strong anti-tumor immune response for two distinct combination therapies. Tumor cells evade immunodestruction by reducing the expression of antigens in their cell membrane [96]. Mutant cells are able to escape destruction due to their resistance to treatment and their low antigenicity, which keeps them from eliciting an immune reaction. The model predictions suggest that treatments aimed at boosting the immune response against a tumor (such as NK cell or CTL adoptive therapy) in patients whose immune system response is anergic, are likely to become an integral part of successful combination therapies.

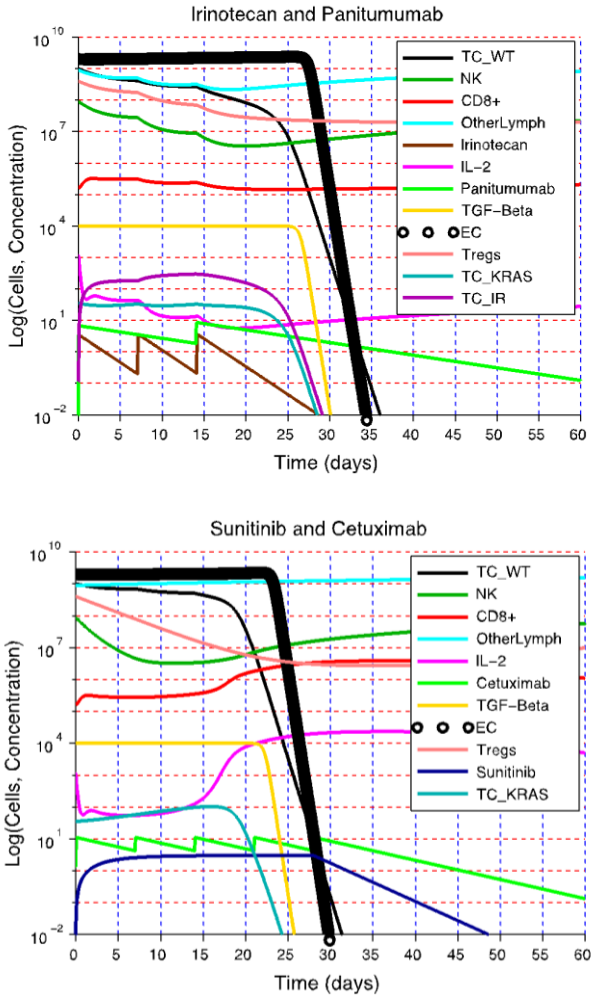

Figure 8. A strong immune response can lead to elimination of resistant tumor cells. A) KRAS-mutant and irinotecan-resistant tumor cells remain vulnerable to immunodestruction if tumor cell antigenicity is high enough and the immune system is capable of a strong response. B) A sunitinib + cetuximab combination therapy is also likely to be therapeutic, leading to the destruction of wild-type and mutant tumor cells. Of note is the fact that in both treatment simulations, a strong immune response reduced the number of injections and sunitinib capsule intake required to eliminate the tumor

3.4. Sensitivity Analysis of the Model Parameters

We performed a sensitivity analysis of the model parameters to identify the parameter(s) that have the greatest influence on the predicted system dynamics. We followed the standard procedure of increasing and decreasing the value of each parameter listed in Table 4 by some percent while leaving all other parameters constant at

the values shown in Supplementary Table 1. The case of no treatment with a moderate immune response and initial tumor size of 10^8 cells was considered. All other initial conditions were left the same as in Table 1. We computed the resulting percent change in the number of tumor cells at steady state (on day 250) after each parameter was increased and decreased by 5%.

Table 4. Sensitivity of Final Tumor Size to a 5% Change to Parameter Values

Parameter	Description	% Change in Tumor Size	
		Parameter decreased by 5%	Parameter increased by 5%
a_w	Tumor growth rate.	-0.028277%	0.025552%
T_K	Carrying capacity of wild-type and mutant tumor cells combined in the absence of tumor angiogenesis.	-0.002276%	0.002276%
α	Rate of circulating lymphocyte production.	0.000593%	-0.000528%
p_1	Maximum rate of production of TGF-β by hypoxic tumor cells.	-1.916486%	1.802060%
b_1	Critical tumor size at which the angiogenic switch occurs.	0.000001%	-0.000001%
S_1	Concentration of TGF-β necessary to reduce the CD8+ T cell killing rate of tumor cells by half.	0.003478%	-0.003187%
w	Rate of Treg cell production.	-0.003755%	0.003613%
b_K	Proliferation rate of angiogenic endothelial cells.	-2.054560%	1.912023%
$K_{\max}$	Maximum carrying capacity for blood vessel growth stimulated by TGF-β.	-3.751997%	3.665944%
e	Rate of NK synthesis.	0.006274%	-0.006108%
r_1	Rate of activation of CD8+ T cell due to NK cell-lysed tumor cell debris.	0.006069%	-0.005907%
r_2	Rate of CD8+ T cell production from circulating lymphocytes.	0.000012%	-0.000012%
j	Rate of activation of CD8+ T cells due to CD8+ T cell-lysed tumor cell debris.	0.0000001%	-0.0000001%
k	Tumor size required for half-maximal CD8+ T cell activation by CD8+ T cell-lysed tumor cell debris.	-0.00000002%	-0.000000008%
ω	Rate of IL-2 production from CD8+ T cells.	-0.026110%	0.023416%
ϕ	Rate of IL-2 production from CD4+ and naive CD8+ T cell IL-2 production.	-0.002137%	0.002107%
p_R	Rate of IL-2-induced Treg cell proliferation.	-0.042878%	0.039535%
d	Immune strength coefficient.	0.026600%	-0.026622%
l	Immune system strength scaling coefficient.	-0.418652%	0.232891%
s	Value describing how quickly CD8+ T cells respond to the presence of a tumor.	-0.027989%	0.025305%

The sensitivity analysis suggests that the model dynamics are robust with respect to slight changes in the parameters values, since the terminal tumor size did not change by more than 5% given a 5% change in the parameter values. Moreover, the parameters that have the greatest influence on the final tumor size are those representing the angiogenic potential of the tumor (K_{max}, b_K and p_1). This result highlights the important role that TGF-β plays in tumor growth and why an anti-TGF- β drug such as Fresolimumab is an essential component of a robust combination treatment.

4. Conclusions

The model simulations presented in this article illustrated the importance of treatment timing and the strength of the anti-tumor immune response in determining the outcome of a treatment. The model analysis helped to identify treatment modalities that are most likely to synergize when given in combination. In particular, a combination of sunitinib and fresolimumab was predicted to be robust with respect to changes in the strength of the immune response, the tumor size at the start of treatment, and with respect to tumor

resistance to cetuximab, panitumumab and irinotecan. This prediction suggests that an effective cancer treatment will be one that can disrupt the biological mechanisms that are responsible for tumor angiogenesis and immunosuppression, which could maximize the therapeutic effect of adoptive cell transfer. In the future, additional cell types and cytokines will be incorporated into the model to take into account the positive feedback loops that lead to anti-tumor and pro-tumor immune cell differentiation and that reinforce pro-tumor and anti-tumor cell phenotypes. The robustness of a cancer treatment with respect to changes in tumor growth rate and antigenicity may depend on the organ in which a cancer develops. Therefore, parameterization of the model with values that are characteristic of a particular cancer type will help to identify the treatment protocols that have the greatest potential to eliminate a specific type of cancer safely and efficiently.

This research did not receive any specific grant from funding agencies in the public, commercial, or not-for-profit sectors.

Appendix

Supplementary Table 1. Parameters of the Model

Parameter	Description	Value	Units	References
a_w	Tumor growth rate (colorectal cancer)	2.31×10^{-1}	day^{-1}	[86]
c	Rate of NK cell-induced tumor death	5.156×10^{-14}	L cell^{-1} day^{-1}	[86]
d	Immune strength coefficient	{1.3, 1.6, 2.1}	day^{-1}	[86]
l	Immune system strength scaling coefficient	{1.1, 1.4, 2}	unitless	[86]
s	Value describing how quickly CD8+ T cells respond to the presence of a tumor	$\{5\times10^{-3}, 8\times10^{-3}, 4\times10^{-2}\}$	L	[86]
ξ	Rate of NK cell-induced tumor death through antibody-dependent cellular cytotoxicity (ADCC)	6.5×10^{-10} (0 for panitumumab)	L cell^{-1} day^{-1}	[86]
h_1	Concentration of mAbs necessary for half-maximal increase in ADCC activity	1.25×10^{-6} (0 for panitumumab)	mg L^{-1}	[86]
X	Determines the percent level of the maximum rate of chemotherapy-induced tumor death of wild-type and mutant cells	0.75	unitless	[86]
K_T	Actual rate of chemotherapy-induced wild-type and mutant tumor cell death used in the simulations	$(8.1\times10^{-1})\cdot X$	day^{-1}	[86,87]
K_{AT}	Additional chemotherapy-induced death of wild-type and mutant tumors due to mAbs cetuximab and panitumumab	4×10^{-4}	L mg^{-1} day^{-1}	[86]
δ_T	Chemotherapy efficacy coefficient on wild-type and mutant cancer cells	2×10^{-1}	L mg^{-1}	[86]
Y	Determines the percent level of the maximum rate of mAb-induced tumor death of wild-type and mutant cells	0.75	unitless	[86]
ψ	Actual rate of mAb-induced wild-type and mutant tumor cell death used in the simulations	$(2.28\times10^{-2})\cdot Y$ for cetuximab $(3.125\times10^{-2})\cdot Y$ for panitumumab	L mg^{-1} day^{-1}	[86]
f	Rate of NK cell turnover	1×10^{-2}	day^{-1}	[86]
e	Rate of NK synthesis	$\frac{1}{9}\cdot f$	day^{-1}	[86]
g_N	IL-2 concentration needed for half-maximal NK cell proliferation	2.5036×10^{5}	IU L^{-1}	[86]
p_N	Rate of IL-2-induced NK cell proliferation	5.13×10^{-2}	day^{-1}	[86]
p	Rate of NK cell death due to interaction with the tumor	5.156×10^{-14}	cell^{-1} day^{-1}	[86]
p_A	Rate of NK cell death due to interaction with mAbs complexes	6.5×10^{-10} (0 for panitumumab)	cell^{-1} day^{-1}	[86]
K_N	Rate of NK cell depletion due to chemotherapy toxicity	9.048×10^{-1}	day^{-1}	[86]

Parameter	Description	Value	Units	References
δ_N	Coefficient of chemotherapy toxicity on NK cells	2×10^{-1}	L mg^{-1}	[86]
m	Rate of turnover of activated CD8+ T cells	5×10^{-3}	day^{-1}	[86]
θ	IL-2 concentration required to halve the CD8+ T cell turnover rate	2.5036×10^{-3}	IU L^{-1}	[86]
q	Rate of CD8+ T cell death due to interaction with the tumor	5.156×10^{-17}	cell^{-1} day^{-1}	[86]
r_1	Rate of activation of CD8+ T cell due to NK cell-lysed tumor cell debris	5.156×10^{-12}	cell^{-1} day^{-1}	[86]
r_2	Rate of CD8+ T cell production from circulating lymphocytes	1×10^{-15}	cell^{-1} day^{-1}	[86]
p_{I_2}	Rate of IL-2 induced CD8+ T cell activation	2.4036	day^{-1}	[86]
g_{I_2}	Concentration of IL-2 necessary for half-maximal CD8+ T cell activation	2.5036×10^{3}	IU L^{-1}	[86]
u	Rate of inhibition of surplus CD8+ T cells induced by Treg cells in the presence of IL-2	2.3085×10^{-13}	L^2 cell^{-2} day^{-1}	[97]
κ	Concentration of IL-2 required to halve the immunosuppressive effect of Treg cells on CD8+ T cells	2.5036×10^{3}	IU L^{-1}	[97]
j	Rate of activation of CD8+ T cells due to CD8+ T cell-lysed tumor cell debris	1.245×10^{-4}	day^{-1}	[86]
k	Tumor size required for half-maximal CD8+ T cell activation by CD8+ T cell-lysed tumor cell debris	2.019×10^{7}	cells	[86]
K_L	Rate of CD8+ T cell depletion from chemotherapy toxicity	4.524×10^{-1}	day^{-1}	[86]
δ_L	Coefficient of chemotherapy toxicity on CD8+ T cells	2×10^{-1}	L mg^{-1}	[86]
β	Rate of lymphocyte turnover	6.3×10^{-3}	day^{-1}	[86]
α	Rate of circulating lymphocyte production	$(3\times10^{9})\cdot\beta$	cells L^{-1} day^{-1}	[86]
K_C	Rate of lymphocyte depletion from chemotherapy toxicity	5.7×10^{-1}	day^{-1}	[86]
δ_C	Coefficient of chemotherapy toxicity on circulating lymphocytes	2×10^{-1}	L mg^{-1}	[86]
μ_{I_2}	Rate of excretion and elimination of IL-2	11.7427	day^{-1}	[86]
ω	Rate of IL-2 production from CD8+ T cells	7.88×10^{-2}	IU cell^{-1} day^{-1}	[86]
ϕ	Rate of IL-2 production from CD4+ and naive CD8+ T cell IL-2 production	1.788×10^{-7}	IU cell^{-1} day^{-1}	[86]
ζ	Concentration of IL-2 for half-maximal CD8+ T cell IL-2 production	2.5036×10^{3}	IU L^{-1}	[86]
γ_1	The rate of excretion and elimination of irinotecan	4.077×10^{-1}	day^{-1}	[86]
η	Rate of cetuximab and panitumumab turnover and excretion	1.386×10^{-1} for cetuximab 9.242×10^{-2} for panitumumab	day^{-1}	[86]
λ	Rate of mAb/tumor cell complex formation	8.9×10^{-14} for cetuximab 8.6×10^{-14} for panitumumab	mg cell^{-1} L^{-1} day^{-1}	[86]
h_2	Concentration of mAbs for half-maximal EGFR binding	4.45×10^{-5} for cetuximab 4.3×10^{-5} for panitumumab	mg L^{-1}	[86]

Parameter	Description	Value	Units	References
T_K	Carrying capacity of wild-type and mutant tumor cells combined in the absence of tumor angiogenesis	1×10^{6}	cells	[88]
g_2	Conversion factor from number of activated endothelial cells to the increase in tumor carrying capacity	1	$\frac{tumor\ cells}{endothelial\ cell}$	estimated
p_1	Maximum rate of production of TGF-β by hypoxic tumor cells	1×10^{5}	IU L^{-1} day^{-1}	estimated from [88]
b_1	Critical tumor size at which the angiogenic switch occurs	1×10^{6}	cells	[88]
S_1	Concentration of TGF-β necessary to reduce the CD8+ T cell killing rate of tumor cells by half	7×10^{4}	IU L^{-1}	[72]
u_1	Decay rate of TGF-β	10	day^{-1}	[88]
b_K	Proliferation rate of angiogenic endothelial cells	0.198	day^{-1}	[98]
$K_{\max}$	Maximum carrying capacity for blood vessel growth stimulated by TGF-β secreted by tumor cells	5×10^{9}	cells	estimated
g_1	TGF-β concentration that gives a half-maximal proliferation rate of endothelial cells	1×10^{4}	IU L^{-1}	estimated
d_K	Growth inhibition coefficient of endothelial cells by tumor cells	5×10^{-8}	$cell^{-2/3}$ day^{-1}	estimated from [99]
λ_T	Suppressive effect of Treg cells on wild-type and mutant tumor cell kill rate by NK cells	1.59×10^{-9}	L $cell^{-1}$	[89]
w	Rate of Treg cell production	4.698×10^{-4}	day^{-1}	[89]
u_R	Rate of Treg cell turnover	3.851×10^{-2}	day^{-1}	[100]
p_R	Rate of IL-2-induced Treg cell proliferation	3.598×10^{-2}	day^{-1}	[97]
g_R	Concentration of IL-2 necessary for half-maximal activation of Treg cells	11.027	IU L^{-1}	[97]
h_R	Rate of Treg cell inhibition by sunitinib	0.227	day^{-1}	[89]
K_R	Rate of Treg cell depletion from chemotherapy toxicity	5.7×10^{-1}	day^{-1}	[86]
α_1	Determines the scope of influence of KRAS-mutant tumor cells T_{cp} in making tumor cells resistant to chemotherapy and in reducing the sensitizing role of cetuximab and panitumumab to chemotherapy	1×10^{7}	unitless	[87]
λ_R	Efficacy of sunitinib in inhibiting the immunosuppressive activity of Treg cells	50.02	L mg^{-1}	[89]
δ_R	Chemotherapy toxicity on Treg cells	2×10^{-1}	L mg^{-1}	[86]
η_S	Rate of excretion and elimination of sunitinib	0.277	day^{-1}	[89]
a_m	Growth rate of mutant tumor cells	2.31×10^{-1}	day^{-1}	[86]
μ	Maximum mutation rate of wild-type tumor cells	4×10^{-5}	day^{-1}	[80]
K_M	Concentration of irinotecan chemotherapy that leads to a half-maximal rate of mutation of wild-type tumor cells T_w into irinotecan-resistant tumor cells T_i	1×10^{3}	mg L^{-1}	estimated
δ_{TR}	Efficacy of the second type of chemotherapy drug of killing irinotecan-resistant tumor cells	2×10^{-1}	L mg^{-1}	[86]
γ_2	Rate of excretion and elimination of the type 2 chemotherapy drug	4.077×10^{-1}	day^{-1}	[86]
η_F	Degradation rate of anti-TGF-beta (Fresolimumab)	0.033	day^{-1}	[70]
b_2	Rate of loss of free TGF-β due to binding with anti-TGF-β	100	L mg^{-1} day^{-1}	[70]
b_3	Rate of loss of free anti-TGF-β due to binding with TGF-β	2.5×10^{-13}	L IU^{-1} day^{-1}	[70]

Supplementary Table 2 lists the outcomes of over 20 simulated anti-cancer treatments under the assumption that tumor cells can stimulate angiogenesis through secretion of TFG-β, and that Treg cells and TGF-β are immunosuppressive. Column 4 corresponds to simulations that assumed no resistance to any treatment. Column 5 correspond to simulations that assumed a presence of 35 KRAS-mutant tumor cells at the start of treatment, and a dose-dependent emergence of irinotecan-resistant tumor cells in treatments that used irinotecan as the cytotoxic agent. Without any treatment, the model predicts that an angiogenic tumor of size up to 1×10^8 cells can be eliminated if a patient's anti-tumor immune response is strong (D_s). IL-2 injections had no effect on tumor growth when administered as monotherapy or as part of a combination therapy. Therefore, combinatorial treatments that involved IL-2 were not included in Supplementary Table 2.

Legend:

I = Irinotecan
C = Cetuximab
P = Panitumumab
S = Sunitinib
F = Fresolimumab
NK = Natural killer cells
CTL = Cytotoxic T lymphocytes
C_2 = Hypothetical chemotherapy drug

Response to treatment:

CR = Complete response: a tumor size at the end of the treatment period that is less than or equal to the diffusion-limited value of 1×10^6 tumor cells.
PR = Partial response: a tumor that remains larger than 1×10^6 cells, but that by the end of the treatment period is smaller than at the start of treatment.
NR = No response: the tumor size remains the same, or becomes larger than it was at the start of treatment, by the time the treatment period ends.

Supplementary Table 2. Simulated Treatments and their Outcomes

Treatment	Immune Strength *D*	Tumor size (# of cells)	Outcome (assuming no treatment resistance)	Outcome (assuming resistance to cetuximab, panitumumab and irinotecan)
None	Strong	10^8	CR	Not applicable
		10^9	NR	Not applicable
	Moderate	10^8	NR	Not applicable
		10^9	NR	Not applicable
	Weak	10^8	NR	Not applicable
		10^9	NR	Not applicable
I	Strong	10^8	CR	CR
		10^9	CR	CR
	Moderate	10^8	NR	NR
		10^9	NR	NR
	Weak	10^8	NR	NR
		10^9	NR	NR
C	Strong	10^8	CR	CR
		10^9	NR	NR
	Moderate	10^8	NR	NR
		10^9	NR	NR
	Weak	10^8	NR	NR
		10^9	NR	NR
P	Strong	10^8	CR	CR
		10^9	CR	CR
	Moderate	10^8	CR	NR
		10^9	NR	NR
	Weak	10^8	CR	NR
		10^9	NR	NR

Treatment	Immune Strength *D*	Tumor size (# of cells)	Outcome (assuming no treatment resistance)	Outcome (assuming resistance to cetuximab, panitumumab and irinotecan)
S	Strong	10^8	CR	CR
		10^9	CR	CR
	Moderate	10^8	NR	NR
		10^9	NR	NR
	Weak	10^8	NR	NR
		10^9	NR	NR
F	Strong	10^8	CR	CR
		10^9	CR	CR
	Moderate	10^8	CR	CR
		10^9	CR	CR
	Weak	10^8	NR	NR
		10^9	NR	NR
NK	Strong	10^8	CR	CR
		10^9	NR	NR
	Moderate	10^8	NR	NR
		10^9	NR	NR
	Weak	10^8	NR	NR
		10^9	NR	NR
CTL	Strong	10^8	CR	CR
		10^9	NR	NR
	Moderate	10^8	NR	NR
		10^9	NR	NR
	Weak	10^8	NR	NR
		10^9	NR	NR
I+C	Strong	10^8	CR	CR
		10^9	NR	NR
	Moderate	10^8	PR	NR
		10^9	NR	NR
	Weak	10^8	NR	NR
		10^9	NR	NR
I+P	Strong	10^8	CR	CR
		10^9	CR	CR
	Moderate	10^8	CR	NR
		10^9	CR	NR
	Weak	10^8	CR	NR
		10^9	CR	NR
I+S	Strong	10^8	CR	CR
		10^9	CR	CR
	Moderate	10^8	CR	CR
		10^9	CR	CR
	Weak	10^8	NR	NR
		10^9	NR	NR
I+F	Strong	10^8	CR	CR
		10^9	CR	CR
	Moderate	10^8	NR	NR
		10^9	NR	NR
	Weak	10^8	NR	NR
		10^9	NR	NR

Treatment	Immune Strength *D*	Tumor size (# of cells)	Outcome (assuming no treatment resistance)	Outcome (assuming resistance to cetuximab, panitumumab and irinotecan)
I+NK	Strong	10^8	CR	CR
		10^9	CR	CR
	Moderate	10^8	CR	CR
		10^9	CR	CR
	Weak	10^8	NR	NR
		10^9	NR	NR
I+CTL	Strong	10^8	CR	CR
		10^9	CR	CR
	Moderate	10^8	CR	CR
		10^9	CR	CR
	Weak	10^8	NR	NR
		10^9	NR	NR
S+C	Strong	10^8	CR	CR
		10^9	CR	CR
	Moderate	10^8	CR	CR
		10^9	CR	CR
	Weak	10^8	PR	NR
		10^9	NR	NR
S+P	Strong	10^8	CR	CR
		10^9	CR	CR
	Moderate	10^8	CR	CR
		10^9	CR	CR
	Weak	10^8	CR	NR
		10^9	CR	NR
S+F (robust)	Strong	10^8	CR	CR
		10^9	CR	CR
	Moderate	10^8	CR	CR
		10^9	CR	CR
	Weak	10^8	CR	CR
		10^9	CR	CR
S+NK	Strong	10^8	CR	CR
		10^9	CR	CR
	Moderate	10^8	NR	NR
		10^9	NR	NR
	Weak	10^8	NR	NR
		10^9	NR	NR
S+CTL	Strong	10^8	CR	CR
		10^9	CR	CR
	Moderate	10^8	NR	NR
		10^9	NR	NR
	Weak	10^8	NR	NR
		10^9	NR	NR
F+C	Strong	10^8	CR	CR
		10^9	CR	CR
	Moderate	10^8	CR	CR
		10^9	CR	CR
	Weak	10^8	CR	NR
		10^9	PR	NR

Treatment	Immune Strength *D*	Tumor size (# of cells)	Outcome (assuming no treatment resistance)	Outcome (assuming resistance to cetuximab, panitumumab and irinotecan)
F+P	Strong	10^8	CR	CR
		10^9	CR	CR
	Moderate	10^8	CR	CR
		10^9	CR	CR
	Weak	10^8	CR	NR
		10^9	CR	NR
F+NK	Strong	10^8	CR	CR
		10^9	CR	CR
	Moderate	10^8	CR	CR
		10^9	CR	CR
	Weak	10^8	NR	NR
		10^9	NR	NR
F+CTL	Strong	10^8	CR	CR
		10^9	CR	CR
	Moderate	10^8	NR	NR
		10^9	NR	NR
	Weak	10^8	NR	NR
		10^9	NR	NR
S+P+NK	Strong	10^8	CR	CR
		10^9	CR	CR
	Moderate	10^8	CR	CR
		10^9	CR	CR
	Weak	10^8	NR	NR
		10^9	NR	NR
$I + C_2$	Strong	10^8	CR	CR
		10^9	CR	CR
	Moderate	10^8	CR	NR
		10^9	CR	NR
	Weak	10^8	CR	NR
		10^9	CR	NR

REFERENCES

[1] Koutsogiannouli E, Papavassiliou AG, Papanikolaou NA. Complexity in cancer biology: is systems biology the answer? Cancer Med. Wiley-Blackwell; 2013; 2: 164–77. doi:10.1002/cam4.62.

[2] Du W, Elemento O. Cancer systems biology: embracing complexity to develop better anticancer therapeutic strategies. Oncogene. 2015; 34: 3215–3225. doi: 10.1038/onc.2014.291.

[3] Félix M-A, Barkoulas M. Pervasive robustness in biological systems. Nat Rev Genet. 2015; 16: 483–496. doi: 10.1038/nrg3949.

[4] Balmain A, Gray J, Ponder B. The genetics and genomics of cancer. Nat Genet. 2003; 33: 238–244. doi:10.1038/ng1107.

[5] O'Connor MJ. Targeting the DNA Damage Response in Cancer. Mol Cell. Elsevier; 2015; 60: 547–60. doi:10.1016/j.molcel.2015.10.040.

[6] van Vugt MATM, Reinhardt HC. Editorial: Cancer-Associated Defects in the DNA Damage Response: Drivers for Malignant Transformation and Potential Therapeutic Targets. Front Genet. 2015;6. doi: 10.3389/fgene.2015.00355.

[7] Goldstein M, Kastan MB. The DNA Damage Response: Implications for Tumor Responses to Radiation and Chemotherapy. Annu Rev Med. 2015; 66: 129–143. doi: 10.1146/annurev-med-081313-121208.

[8] Astolfi L, Ghiselli S, Guaran V, Chicca M, Simoni E, Olivetto E, et al. Correlation of adverse effects of cisplatin administration in patients affected by solid tumours: a retrospective evaluation. Oncol Rep. 2013; 29: 1285–92. doi: 10.3892/or.2013.2279.

[9] Elice F, Rodeghiero F. Side effects of anti-angiogenic drugs. Thromb Res. 2012; 129: S50–S53. doi: 10.1016/S0049-3848(12)70016-6.

[10] Baldo B. Adverse events to monoclonal antibodies used for

cancer therapy: Focus on hypersensitivity responses. Oncoimmunology. 2013; 2: e26333. doi: 10.4161/onci.26333.

[11] Andrews S, Holden R. Characteristics and management of immunerelated adverse effects associated with ipilimumab, a new immunotherapy for metastatic melanoma. Cancer Manag Res. Dove Press; 2012; 4: 299–307. doi:10.2147/CMAR.S31873.

[12] DeVita VT, Chu E. A History of Cancer Chemotherapy. Cancer Res. 2008; 68.

[13] Nitiss JL. Targeting DNA topoisomerase II in cancer chemotherapy. Nat Rev Cancer. NIH Public Access; 2009;9: 338–50. doi: 10.1038/nrc2607.

[14] Ewesuedoa R, Ratain M. Topoisomerase I Inhibitors. Oncologist. 1997; 2: 359–364.

[15] Dwarakanath BS, Khaitan D, Mathur R. Inhibitors of topoisomerases as anticancer drugs: problems and prospects. Indian J Exp Biol. 2004; 42: 649–59. Available: http://www.ncbi.nlm.nih.gov/pubmed/15339028.

[16] Alfarouk KO, Stock C-M, Taylor S, Walsh M, Muddathir AK, Verduzco D, et al. Resistance to cancer chemotherapy: failure in drug response from ADME to P-gp. Cancer Cell Int. BioMed Central; 2015; 15: 71. doi: 10.1186/s12935-015-0221-1.

[17] Mellor HR, Callaghan R. Resistance to chemotherapy in cancer: a complex and integrated cellular response. Pharmacology. Karger Publishers; 2008; 81: 275–300. doi: 10.1159/000115967.

[18] Ferrara N, Hillan KJ, Gerber H-P, Novotny W. Case history: Discovery and development of bevacizumab, an anti-VEGF antibody for treating cancer. Nat Rev Drug Discov. Nature Publishing Group; 2004; 3: 391–400. doi:10.1038/nrd1381.

[19] Meadows KL, Hurwitz HI. Anti-VEGF therapies in the clinic. Cold Spring Harb Perspect Med. Cold Spring Harbor Laboratory Press; 2012; 2. doi: 10.1101/cshperspect.a006577.

[20] Morris JC, Tan AR, Olencki TE, Shapiro GI, Dezube BJ, Reiss M, et al. Phase I study of GC1008 (fresolimumab): a human anti-transforming growth factor-beta (TGFβ) monoclonal antibody in patients with advanced malignant melanoma or renal cell carcinoma. PLoS One. Public Library of Science; 2014; 9: e90353. doi: 10.1371/journal.pone.0090353.

[21] Sheen YY, Kim M-J, Park S-A, Park S-Y, Nam J-S. Targeting the Transforming Growth Factor-β Signaling in Cancer Therapy. Biomol Ther (Seoul). Korean Society of Applied Pharmacology; 2013; 21: 323–31. doi:10.4062/biomolther.2013.072.

[22] Xu W, Yang Z, Lu N, Guggenheim D, Shah M, Rahman R, et al. Molecular targeted therapy for the treatment of gastric cancer. J Exp Clin Cancer Res. BioMed Central; 2016; 35: 1. doi: 10.1186/s13046-015-0276-9.

[23] Lindberg JM, Newhook TE, Adair SJ, Walters DM, Kim AJ, Stelow EB, et al. Co-treatment with panitumumab and trastuzumab augments response to the MEK inhibitor trametinib in a patient-derived xenograft model of pancreatic cancer. Neoplasia. Neoplasia Press; 2014; 16: 562–71. doi: 10.1016/j.neo.2014.06.004.

[24] Gutheil JC, Campbell TN, Pierce PR, Watkins JD, Huse WD, Bodkin DJ, et al. Targeted Antiangiogenic Therapy for Cancer Using Vitaxin: A Humanized Monoclonal Antibody to the Integrin alphavbeta3. Clin Cancer Res. 2000; 6: 3056–3061.

[25] Liu Z, Wang F, Chen X. Integrin alpha(v)beta(3)-Targeted Cancer Therapy. Drug Dev Res. NIH Public Access; 2008; 69: 329–339. doi: 10.1002/ddr.20265.

[26] Salas RN, Finke JH, Rini BI. The intersection of sunitinib with the immunosuppressive microenvironment of renal cell carcinoma: implications for future therapeutics. Target Oncol. Springer-Verlag; 2007; 2: 225–234. doi:10.1007/s11523-007-0064-3.

[27] Lindau D, Gielen P, Kroesen M, Wesseling P, Adema GJ. The immunosuppressive tumour network: myeloid-derived suppressor cells, regulatory T cells and natural killer T cells. Immunology. 2013; 138: 105–15. doi:10.1111/imm.12036.

[28] Fujimura T, Kambayashi Y, Aiba S. Crosstalk between regulatory T cells (Tregs) and myeloid derived suppressor cells (MDSCs) during melanoma growth. Oncoimmunology. Taylor & Francis; 2012; 1: 1433–1434. doi:10.4161/onci.21176.

[29] Coulson A, Levy A, Gossell-Williams M. Monoclonal Antibodies in Cancer Therapy: Mechanisms, Successes and Limitations. West Indian Med J. The University of the West Indies; 2014;63: 650–4. doi:10.7727/wimj.2013.241.

[30] Farid SS. Process economics of industrial monoclonal antibody manufacture. J Chromatogr B Analyt Technol Biomed Life Sci. 2007; 848: 8–18. doi:10.1016/j.jchromb.2006.07.037.

[31] Rudnick SI, Adams GP. Affinity and avidity in antibody-based tumor targeting. Cancer Biother Radiopharm. Mary Ann Liebert, Inc.; 2009; 24: 155–61. doi:10.1089/cbr.2009.0627.

[32] Thurber GM, Schmidt MM, Wittrup KD. Antibody tumor penetration: transport opposed by systemic and antigen-mediated clearance. Adv Drug Deliv Rev. NIH Public Access; 2008; 60: 1421–34. doi:10.1016/j.addr.2008.04.012.

[33] Altan M, Burtness B, Arteaga C, Engelman J, Burtness B, Goldwasser M, et al. EGFR-directed antibodies increase the risk of severe infection in cancer patients. BMC Med. BioMed Central; 2015; 13: 37. doi:10.1186/s12916-015-0276-9.

[34] Kollmannsberger C, Soulieres D, Wong R, Scalera A, Gaspo R, Bjarnason G. Sunitinib therapy for metastatic renal cell carcinoma: recommendations for management of side effects. Can Urol Assoc J. Canadian Medical Association; 2007; 1: S41-54. Available: http://www.ncbi.nlm.nih.gov/pubmed/18542784.

[35] Morton RF, Hammond EH. ASCO Provisional Clinical Opinion: KRAS, Cetuximab, and Panitumumab-Clinical Implications in Colorectal Cancer. J Oncol Pract. American Society of Clinical Oncology; 2009; 5: 71–2. doi:10.1200/JOP.0924603.

[36] Tan C, Du X. KRAS mutation testing in metastatic colorectal cancer. World J Gastroenterol. Baishideng Publishing Group Inc; 2012; 18: 5171–80. doi:10.3748/wjg.v18.i37.5171.

[37] El Guerrab A, Bamdad M, Kwiatkowski F, Bignon Y-J, Penault-Llorca F, Aubel C. Anti-EGFR monoclonal antibodies and EGFR tyrosine kinase inhibitors as combination therapy for triple-negative breast cancer. Oncotarget. 2016; doi:10.18632/oncotarget.12037.

[38] Zhang F, Yu Y, Xing L, Chen M. Cetuximab combined with chemotherapy is beneficial for patients with advanced non-small cell lung cancer after EGFR-tyrosine kinase inhibitors failure. Int J Clin Exp Med. e-Century Publishing Corporation; 2015; 8: 16140–8. Available: http://www.ncbi.nlm.nih.gov/pubmed/26629127.

[39] Carrato A, Gómez A, Escudero P, Chaves M, Rivera F, Marcuello E, et al. Panitumumab and irinotecan every 3 weeks is an active and convenient regimen for second-line treatment of patients with wild-type K-RAS metastatic colorectal cancer. Clin Transl Oncol. Springer Milan; 2013; 15: 705–711. doi:10.1007/s12094-012-0993-x.

[40] Van Emburgh BO, Sartore-Bianchi A, Di Nicolantonio F, Siena S, Bardelli A, Adam R, et al. Acquired resistance to EGFR-targeted therapies in colorectal cancer. Mol Oncol. Elsevier; 2014; 8: 1084–94. doi:10.1016/j.molonc.2014.05.003.

[41] Hsu H-C, Thiam TK, Lu Y-J, Yeh CY, Tsai W-S, You JF, et al. Mutations of KRAS/NRAS/BRAF predict cetuximab resistance in metastatic colorectal cancer patients. Oncotarget. 2016; 7: 22257–70. doi:10.18632/oncotarget.8076.

[42] Braig F, März M, Schieferdecker A, Schulte A, Voigt M, Stein A, et al. Epidermal growth factor receptor mutation mediates cross-resistance to panitumumab and cetuximab in gastrointestinal cancer. Oncotarget. 2015; 6: 12035–47. doi: 10.18632/oncotarget.3574.

[43] Petitprez A, Poindessous V, Ouaret D, Regairaz M, Bastian G, Guérin E, et al. Acquired irinotecan resistance is accompanied by stable modifications of cell cycle dynamics independent of MSI status. Int J Oncol. 2013; 42: 1644–53. doi:10.3892/ijo.2013.1868.

[44] Dowling JK, Mansell A. Toll-like receptors: the swiss army knife of immunity and vaccine development. Clin Transl Immunol. Nature Publishing Group; 2016; 5: e85. doi: 10.1038/cti.2016.22.

[45] Wang N, Liang H, Zen K. Molecular mechanisms that influence the macrophage m1-m2 polarization balance. Front Immunol. Frontiers Media SA; 2014; 5: 614. doi: 10.3389/fimmu.2014.00614.

[46] Jack CS, Arbour N, Blain M, Meier U-C, Prat A, Antel JP. Th1 polarization of CD4+ T cells by Toll-like receptor 3-activated human microglia. J Neuropathol Exp Neurol. 2007; 66: 848–59. doi: 10.1097/nen.0b013e3181492a7.

[47] Tugues S, Burkhard SH, Ohs I, Vrohlings M, Nussbaum K, vom Berg J, et al. New insights into IL-12-mediated tumor suppression. Cell Death Differ. Nature Publishing Group; 2015; 22: 237–246. doi: 10.1038/cdd.2014.134.

[48] Rosenberg SA. IL-2: the first effective immunotherapy for human cancer. J Immunol. American Association of Immunologists; 2014; 192: 5451–8. doi: 10.4049/jimmunol.1490019.

[49] Ferrantini M, Capone I, Belardelli F. Interferon-α and cancer: Mechanisms of action and new perspectives of clinical use. Biochimie. 2007; 89: 884–893. doi: 10.1016/j.biochi.2007.04.006.

[50] Lee S, Margolin K. Cytokines in Cancer Immunotherapy. Cancers (Basel). 2011;3: 3856–3893. doi:10.3390/cancers3043856.

[51] June CH. Adoptive T cell therapy for cancer in the clinic. J Clin Invest. American Society for Clinical Investigation; 2007; 117: 1466–76. doi:10.1172/JCI32446.

[52] Houot R, Schultz LM, Elien Marabelle A, Kohrt H. T-cell–based Immunotherapy: Adoptive Cell Transfer and Checkpoint Inhibition. Cancer Immunol Res. 3: 1115–22. doi: 10.1158/2326-6066.CIR-15-0190.

[53] Lim O, Jung MY, Hwang YK, Shin E-C. Present and Future of Allogeneic Natural Killer Cell Therapy. Front Immunol. Frontiers Media SA; 2015; 6: 286. doi: 10.3389/fimmu.2015.00286.

[54] Dahlberg CIM, Sarhan D, Chrobok M, Duru AD, Alici E. Natural Killer Cell-Based Therapies Targeting Cancer: Possible Strategies to Gain and Sustain Anti-Tumor Activity. Front Immunol. Frontiers Media SA; 2015; 6: 605. doi: 10.3389/fimmu.2015.00605.

[55] Sadelain M, Brentjens R, Rivière I. The basic principles of chimeric antigen receptor (CAR) design. Cancer Discov. NIH Public Access; 2013;3: 388–98. doi:10.1158/2159-8290.CD-12-0548.

[56] Curran KJ, Pegram HJ, Brentjens RJ. Chimeric antigen receptors for T cell immunotherapy: current understanding and future directions. J Gene Med. NIH Public Access; 2012; 14: 405–15. doi:10.1002/jgm.2604.

[57] Newick K, Moon E, Albelda SM, Topalian S, Drake C, Pardoll D, et al. Chimeric antigen receptor T-cell therapy for solid tumors. Mol Ther — Oncolytics. Nature Publishing Group; 2016; 3: 16006. doi:10.1038/mto.2016.6.

[58] Lutsiak MEC, Semnani RT, De Pascalis R, Kashmiri SVS, Schlom J, Sabzevari H. Inhibition of CD4+25+ T regulatory cell function implicated in enhanced immune response by low-dose cyclophosphamide. Blood. 2005; 105: 2862–2868.

[59] Alizadeh D, Larmonier N. Chemotherapeutic targeting of cancer-induced immunosuppressive cells. Cancer Res. NIH Public Access; 2014; 74: 2663–8. doi: 10.1158/0008-5472.CAN-14-0301.

[60] Zitvogel L, Apetoh L, Ghiringhelli F, Kroemer G. Immunological aspects of cancer chemotherapy. Nat Rev Immunol. 2008; 8: 59–73. doi: 10.1038/nri2216.

[61] Chmielewski M, Abken H. TRUCKs: the fourth generation of CARs. Expert Opin Biol Ther. 2015; 15: 1145–1154. doi: 10.1517/14712598.2015.1046430.

[62] Zhang H, Ye Z-L, Yuan Z-G, Luo Z-Q, Jin H-J, Qian Q-J. New Strategies for the Treatment of Solid Tumors with CAR-T Cells. Int J Biol Sci. Ivyspring International Publisher; 2016; 12: 718–29. doi:10.7150/ijbs.14405.

[63] Prosser ME, Brown CE, Shami AF, Forman SJ, Jensen MC. Tumor PD-L1 co-stimulates primary human CD8+ cytotoxic T cells modified to express a PD1:CD28 chimeric receptor. Mol Immunol. 2012; 51: 263–272. doi: 10.1016/j.molimm.2012.03.023.

[64] Kitano H. Biological robustness. Nat Rev Genet. Nature Publishing Group; 2004; 5: 826–837. doi: 10.1038/nrg1471.

[65] Kreeger PK, Lauffenburger DA. Cancer systems biology: a network modeling perspective. Carcinogenesis. Oxford University Press; 2010; 31: 2–8. doi:10.1093/carcin/bgp261.

[66] Folkman J. Tumor angiogenesis: therapeutic implications. N Engl J Med. 1971; 285: 1182–6. doi: 10.1056/NEJM197111182852108.

[67] Xu J, Vilanova G, Gomez H, Folkman J, Hicklin D, Ellis L, et al. A Mathematical Model Coupling Tumor Growth and Angiogenesis. Oberai AA, editor. PLoS One. Public Library of Science; 2016; 11: e0149422. doi: 10.1371/journal.pone.0149422.

[68] Gevertz JL, Torquato S. Modeling the effects of vasculature evolution on early brain tumor growth. J Theor Biol. 2006; 243: 517–31. doi:10.1016/j.jtbi.2006.07.002.

[69] Peirce SM. Computational and mathematical modeling of angiogenesis. Microcirculation. NIH Public Access; 2008;15: 739–51. doi:10.1080/10739680802220331.

[70] Cameron MA, Davis AL, Kostelich E, Eikenberry S. A Mathematical Model of Angiogenesis in Glioblastoma Multiforme [Internet]. Arizona State University. 2009. Available: http://stanford.edu/~mary32/GBM_Paper.pdf.

[71] Soto-Ortiz L, Finley SD. A cancer treatment based on synergy between anti-angiogenic and immune cell therapies. J Theor Biol. 2016; 394: 197–211. doi:10.1016/j.jtbi.2016.01.026.

[72] Robertson-Tessi M, El-Kareh A, Goriely A. A mathematical model of tumor-immune interactions. J Theor Biol. 2012; 294: 56–73. doi:10.1016/j.jtbi.2011.10.027.

[73] Wilkie KP. A review of mathematical models of cancer-immune interactions in the context of tumor dormancy. Adv Exp Med Biol. 2013; 734: 201–34. doi: 10.1007/978-1-4614-1445-2_10.

[74] Eftimie R, Bramson JL, Earn DJD. Interactions Between the Immune System and Cancer: A Brief Review of Non-spatial Mathematical Models. Bull Math Biol. Springer-Verlag; 2011; 73: 2–32. doi:10.1007/s11538-010-9526-3.

[75] Den Breems NY, Eftimie R. The re-polarisation of M2 and M1 macrophages and its role on cancer outcomes. J Theor Biol. 2016; 390: 23–39.

[76] Kogan Y, Agur Z, Elishmereni M. A Mathematical Model for the Immunotherapeutic Control of the Th1/Th2 Imbalance in Melanoma. Dyn Syst Ser B. 2013; 18: 1017–1030. doi:10.3934/dcdsb.2013.18.1017.

[77] Araujo RP, Petricoin EF, Liotta LA. A mathematical model of combination therapy using the EGFR signaling network. Biosystems. 2005; 80: 57–69. doi:10.1016/j.biosystems.2004.10.002.

[78] Callahan MK. Two Drugs Are Better than One—Modeling Drug Combinations in Cancer Therapy. Sci Transl Med. 2013; 5.

[79] Bozic I, Reiter JG, Allen B, Antal T, Chatterjee K, Shah P, et al. Evolutionary dynamics of cancer in response to targeted combination therapy. Elife. eLife Sciences Publications Limited; 2013; 2: e00747. doi: 10.7554/eLife.00747.

[80] Sun X, Bao J, Shao Y, Camidge DR, Pao W, Sequist L V., et al. Mathematical Modeling of Therapy-induced Cancer Drug Resistance: Connecting Cancer Mechanisms to Population Survival Rates. Sci Rep. Nature Publishing Group; 2016; 6: 22498. doi: 10.1038/srep22498.

[81] Tomasetti C, Levy D. An elementary approach to modeling drug resistance in cancer. Math Biosci Eng. NIH Public Access; 2010; 7: 905–18. Available: http://www.ncbi.nlm.nih.gov/pubmed/21077714.

[82] Panetta JC. A Mathematical Model of Drug Resistance: Heterogeneous Tumors. Math Biosci. 1998; 147: 41–61.

[83] De Pillis LG, Radunskaya AE, Wiseman CL. A Validated Mathematical Model of Cell-Mediated Immune Response to Tumor Growth. Cancer Res. 2005; 65: 7950–8. doi: 10.1158/0008-5472.CAN-05-0564.

[84] Kirschner D, Panetta JC. Modeling immunotherapy of the tumor – immune interaction. J Math Biol. 1998; 37: 235–252.

[85] Kim PS, Lee PP, Nestle F, Tonel G, Farkas A, Jaini R, et al. Modeling Protective Anti-Tumor Immunity via Preventative Cancer Vaccines Using a Hybrid Agent-based and Delay Differential Equation Approach. Beerenwinkel N, editor. PLoS Comput Biol. Public Library of Science; 2012; 8: e1002742. doi:10.1371/journal.pcbi.1002742.

[86] dePillis LG, Savage H, Radunskaya AE. Mathematical Model of Colorectal Cancer with Monoclonal Antibody Treatments. Br J Med Med Res. 2014; 4. doi:http://dx.doi.org/10.9734/bjmmr/2014/8393.

[87] Sameen S, Barbuti R, Milazzo P, Cerone A, Del Re M, Danesi R. Mathematical modeling of drug resistance due to KRAS mutation in colorectal cancer. J Theor Biol. 2016; 389: 263–273. doi:10.1016/j.jtbi.2015.10.019.

[88] Arciero JC, Jackson TL, Kirschner De. a Mathematical Model of Tumor-Immune Evasion and Sirna Treatment. Discret Contin Dyn Syst - Ser B. 2004;4: 39–58. Available: http://aimsciences.org.

[89] DePillis L, Caldwell T, Sarapata E, Williams H. Mathematical modeling of regulatory T cell effects on renal cell carcinoma treatment. Discret Contin Dyn Syst - Ser B. 2013; 18: 915–943. doi:10.3934/dcdsb.2013.18.915.

[90] Liu C-Z, Zhang L, Chang X-H, Cheng Y-X, Cheng H-Y, Ye X, et al. Overexpression and immunosuppressive functions of transforming growth factor 1, vascular endothelial growth factor and interleukin-10 in epithelial ovarian cancer. Chin J Cancer Res. Beijing Institute for Cancer Research; 2012; 24: 130–7. doi:10.1007/s11670-012-0130-y.

[91] De Pillis LG, Radunskaya A. A mathematical model of immune response to tumor invasion. Second MIT Conference on Computational Fluid and Solid Mechanics. 2003. pp. 1661–1668.

[92] Sakamoto N, Ishikawa T, Kokura S, Okayama T, Oka K, Ideno M, et al. Phase I clinical trial of autologous NK cell therapy using novel expansion method in patients with advanced digestive cancer. J Transl Med. BioMed Central; 2015; 13: 277. doi:10.1186/s12967-015-0632-8.

[93] Kronik N, Kogan Y, Vainstein V, Agur Z. Improving

alloreactive CTL immunotherapy for malignant gliomas using a simulation model of their interactive dynamics. Cancer Immunol Immunother. 2008; 57: 425–39. doi: 10.1007/s00262-007-0387-z

[94] Kim KS, Cho G, Jung IH. Optimal treatment strategy for a tumor model under immune suppression. Comput Math Methods Med. 2014;2014: 206287. doi: 10.1155/2014/206287.

[95] Welink J, Boven E, Vermorken JB, Gall HE, van der Vijgh WJ. Pharmacokinetics and pharmacodynamics of lobaplatin (D-19466) in patients with advanced solid tumors, including patients with impaired renal of liver function. Clin Cancer Res. 1999; 5: 2349–58. Available: http://www.ncbi.nlm.nih.gov/pubmed/10499604.

[96] Rabinovich GA, Gabrilovich D, Sotomayor EM. Immunosuppressive strategies that are mediated by tumor cells. Annu Rev Immunol. NIH Public Access; 2007; 25: 267–96. doi:10.1146/annurev.immunol.25.022106.141609.

[97] de Pillis L, Fister KR, Gu W, Collins C, Daub M, Gross D, et al. Mathematical Model Creation for Cancer Chemo-Immunotherapy. Comput Math Methods Med. Hindawi Publishing Corporation; 2009; 10: 165–184. doi:10.1080/17486700802216301.

[98] Bian X, Jiang X, Chen J, Bai J, Dai C, Wang Q, et al. Increased angiogenic capabilities of endothelial cells from microvessels of malignant human gliomas. Int Immunopharmacol. 2006; 6: 90–9. doi:10.1016/j.intimp.2005.08.004.

[99] Hahnfeldt P, Panigrahy D, Folkman J, Hlatky L. Tumor development under angiogenic signaling: a dynamical theory of tumor growth, treatment response, and postvascular dormancy. Cancer Res. 1999; 59: 4770–5. Available: http://www.ncbi.nlm.nih.gov/pubmed/10519381.

[100] Mabarrack NHE, Turner NL, Mayrhofer G. Recent thymic origin, differentiation, and turnover of regulatory T cells. J Leukoc Biol. 2008; 84: 1287–97. doi:10.1189/jlb.0308201.